



HAL
open science

Comparison of enrichment methods for efficient nitrogen fixation on a biocathode

Axel Rous, Gaëlle Santa-Catalina, Elie Desmond-Le Quémener, Eric Trably,
Nicolas Bernet

► **To cite this version:**

Axel Rous, Gaëlle Santa-Catalina, Elie Desmond-Le Quémener, Eric Trably, Nicolas Bernet. Comparison of enrichment methods for efficient nitrogen fixation on a biocathode. 2023. hal-04180139

HAL Id: hal-04180139

<https://hal.inrae.fr/hal-04180139>

Preprint submitted on 11 Aug 2023

HAL is a multi-disciplinary open access archive for the deposit and dissemination of scientific research documents, whether they are published or not. The documents may come from teaching and research institutions in France or abroad, or from public or private research centers.

L'archive ouverte pluridisciplinaire **HAL**, est destinée au dépôt et à la diffusion de documents scientifiques de niveau recherche, publiés ou non, émanant des établissements d'enseignement et de recherche français ou étrangers, des laboratoires publics ou privés.



Distributed under a Creative Commons Attribution 4.0 International License

1
2
3
4
5
6
7
8
9
10
11
12
13
14
15
16
17
18
19
20
21
22
23
24
25
26
27
28
29
30
31
32
33
34
35
36
37
38

Comparison of enrichment methods for efficient nitrogen fixation on a biocathode

Axel Rous¹, Gaëlle Santa-Catalina¹, Elie Desmond-Le Quémener¹, Eric Trably¹, Nicolas Bernet¹

¹ INRAE, Univ Montpellier, LBE, 102 avenue des Étangs, 11100 Narbonne, France

*Corresponding author

Correspondence: nicolas.bernet@inrae.fr

ABSTRACT

The production of nitrogen fertilizers in modern agriculture is mostly based on the Haber-Bosch process, representing nearly 2% of the total energy consumed in the world. Low-energy bioelectrochemical fixation of N₂ to microbial biomass was previously observed but the mechanisms of microbial interactions in N₂-fixing electroactive biofilms are still poorly understood. The present study aims to develop a new method of enrichment of autotrophic and diazotrophic bacteria from soil samples with a better electron source availability than using H₂ alone. The enrichment method was based on a multi-stage procedure. The first enrichment step was specifically designed for the selection of N₂-fixing bacteria from soil samples with organic C as electron and carbon source. Then, a polarized cathode was used for the enrichment of autotrophic bacteria using H₂ (hydrogenotrophic) or the cathode as electron source. This enrichment was compared with an enrichment culture of pure diazotrophic hydrogenotrophic bacteria without the use of a microbial electrochemical system. Interestingly, both methods showed comparable results for N₂ fixation rates at day 340 of the enrichment with an estimated average of approximately 0.2 mgN_{fixed}/L.d. Current densities up to -15 A/m² were observed in the polarized cathode enrichments and a significant increase of the microbial biomass on the cathode was shown between 132 and 214 days of enrichment. These results confirmed an enrichment in autotrophic and diazotrophic bacteria on the polarized cathode. It was hypothesised that autotrophic bacteria were able to use either the H₂ produced at the cathode or directly the cathode through direct electron transfer (DET) as more biomass was produced than with H₂ alone. Finally, the analysis of the enriched communities suggested that *Desulforamulus ruminis* mediated microbial interactions between autotrophic anaerobic and heterotrophic aerobic bacteria in polarized cathode enrichment. These interactions could play a key role in the development of biomass in these systems and on N₂ fixation. Based on these findings, a conceptual model on the functioning of mixed cultures N₂-fixing electroactive biofilms was proposed.

39 **Keywords:** Nitrogen fixation, Microbial electrochemical system, Biomass electrostimulation,
40 Enrichment method

41

42

43

Introduction

45 Nitrogen is one of the essential elements for the growth of all living organisms, especially for cellular
46 protein synthesis. In modern agriculture, ammonia is often used as a nitrogen source for plants (Bagali,
47 2012; Burris & Roberts, 1993; Masclaux-Daubresse et al., 2010). This compound is produced at industrial
48 scale by the Haber-Bosch process which allows the reduction of N_2 to NH_3 at the expense of large quantities
49 of H_2 and energy (Kandemir et al., 2013; Martín et al., 2019). This process is associated with significant CO_2
50 emissions, due to the source of H_2 obtained either by methane steam reforming or coal gasification (Martín
51 et al., 2019). Alternatives for green H_2 production, such as water electrolysis, are therefore nowadays
52 considered to feed the Haber-Bosch process that is also contributing to a high energy demand of the
53 process (Cherkasov et al., 2015). A more direct alternative is to reduce N_2 directly on a cathode by chemical
54 catalysts. However, these catalysts are not renewable and are currently not sufficiently selective regarding
55 the hydrogen evolution reaction at ambient conditions (Deng et al., 2018; A. Liu et al., 2020).

56 Recently some authors proposed to use N_2 -fixing bacteria in association with electrochemical systems
57 for N_2 reduction at low energy cost (C. Liu et al., 2017; Rago et al., 2019). This idea was inspired by previous
58 observations of microbial CO_2 fixation on microbial cathodes in a process known as microbial
59 electrosynthesis (A. Liu et al., 2020; Logan et al., 2019). The microbial fixation of both N_2 and CO_2 with a
60 polarized cathode was demonstrated in two recent studies (C. Liu et al., 2017; Rago et al., 2019). First, Liu
61 et al. (2017) demonstrated the growth of *Xanthobacter autotrophicus* in a hybrid organic-inorganic
62 electrochemical system in the absence of nitrogen sources other than N_2 . Then, Rago et al. (2019)
63 demonstrated N_2 fixation through microbial electrosynthesis (MES) with a mixed microbial community (C.
64 Liu et al., 2017; Rago et al., 2019).

65 Other works investigated the mechanisms with pure bacterial strain like Soundararajan et al. (2019)
66 and Chen et al. (2020) with *Rhodopseudomonas palustris* and *Pseudomonas stutzeri* (Chen et al., 2020;
67 Soundararajan et al., 2019). Yadav et al. (2022) demonstrated the possible use of N_2 -fixing bacteria as
68 nitrogen source in a microbial electrosynthesis process of acetate (Yadav et al., 2022). Zhang et al. (2022)
69 also worked on a system of N_2 fixation in microbial electrolysis cell (MEC) (Zhang et al., 2022). In these
70 works, the authors investigated the interactions existing between CO_2 and N_2 fixation microbial processes.
71 Coupling capabilities of N_2 fixation in bioelectrochemical systems as possible source of nitrogen for other
72 biological systems was subject of interest. Indeed, such coupling can lead to the production of molecules
73 of interest such as acetate by reducing the environmental impact of the use of reactive nitrogen often in
74 the form of NH_4Cl (Yadav et al., 2022). The work of Li et al. (2022) in a single-chamber system and
75 highlighted an importance of synergy within an N_2 -fixing community in a microbial bioremediation system
76 (Li et al., 2022).

77 All this work has demonstrated that it is possible to use a cathode as an electron source for biomass
78 growth by fixing N_2 and CO_2 . This biomass could then be used as a fertilizer with a low impact on the
79 environment (Chakraborty & Akhtar, 2021; Rago et al., 2019; y. Hafeez et al., 2006). Although the proof of
80 concept was made for this process, the microbial interactions supporting N_2 fixation in this microbial
81 electrochemical systems are still poorly understood. Different N_2 fixation scenarios are indeed possible,
82 such as: (i) fixation by a single population capable of fixing N_2 and CO_2 using the electrode as sole electron
83 source, (ii) fixation by heterotrophic diazotrophic bacteria that can utilize the organic carbon produced by
84 electro-autotrophic bacteria, (iii) fixation through an interaction between methanogenic archaea and
85 methanotrophs that could use CH_4 as an energy source for N_2 fixation and (iv) fixation through an
86 interaction mediated by direct interspecies electron transfer (DIET) between electro-autotrophic bacteria
87 and diazotrophic bacteria (Rago et al., 2019). A better understanding of these interactions is essential to
88 optimize N_2 fixation in microbial electrochemical system.

89 In nature, biological N_2 fixation is a key mechanism of the nitrogen cycle where atmospheric nitrogen
90 is uptaken by living organisms (Bagali, 2012). It is carried out by so-called diazotrophic bacteria responsible
91 for the transformation of N_2 into NH_3 (Kim & Rees, 1994). Some of these bacteria can be found on the roots
92 of plants where they are living in symbiosis (Burris & Roberts, 1993; Franche et al., 2009). These
93 microorganisms are able to fix N_2 from the air, making it assimilable in the form of NH_4^+ or amino acids (L-
94 glutamine, L-glutamate) which are further used in plants for protein or DNA synthesis (Burris & Roberts,
95 1993). In exchange, the bacteria use the organic matter of root exudates produced by the plants as carbon
96 and energy sources. Among the diazotrophic bacteria, the genera *Frankia* and *Rhizobium spp.* are often

97 associated with leguminous plant roots (Burris & Roberts, 1993; Peoples & Craswell, 1992). In contrast,
98 other free-living N₂-fixing bacteria such as *Azospirillum*, are able to fix N₂ with or without interacting with
99 plants and can use organic or inorganic materials to produce their own energy (Tilak et al., 1986).

100 In order to better understand the microbial mechanisms supporting N₂ fixation in polarized cathode
101 enrichment and produce biomass, this work aims at developing an enrichment method of cathodic biofilms
102 for direct fixation of CO₂ and N₂. Rago et al. (2019) demonstrated the capacity of producing biomass from
103 air, CO₂ and a solid electrode polarized negatively (Rago et al., 2019). Here a specific enrichment of
104 microorganisms capable of N₂ fixation was developed. It was hypothesized that a multi-step enrichment
105 with specific medium could select a microbial community able to fix N₂ and CO₂ supported by electrons
106 brought by a cathode. It was assumed that these communities enriched by this procedure could use a large
107 number of interactions leading to N₂ fixation and biomass growth. For that, it was assumed that the
108 enrichment in autotrophic diazotrophic bacteria in the presence of a cathode with pre-enrichment steps
109 in presence of several electron donors (organic C and cathode) would be more efficient than enrichment
110 cultures of hydrogenotrophic and diazotrophic bacteria. For this, soil samples were used as sources of N₂-
111 fixing bacteria, and successive enrichments in autotrophic bacteria in polarized cathode enrichment (PCE)
112 were performed to select a electroactive biofilm capable of fixing N₂ and CO₂ with a cathode as sole
113 electron source. The enriched biofilm was compared with a classical enrichment of N₂-fixing hydrogen-
114 oxidizing bacteria (HOB) in flasks (named H₂ enrichment, H₂E) (X. Hu et al., 2020; C. Liu et al., 2017).

115 **Methods**

116 **Inoculum**

117 Soil samples from a forest, agricultural crop field and a commercial compost were used as microbial
118 inoculum sources. Samples were collected from forest and agricultural soils in the Haute Vallée de l'Aude,
119 France. These sources were selected based on their assumed abundance of N₂-fixing bacteria and their
120 theoretical C/N ratio (Khan et al., 2016). One to two mg of each samples were used as inoculum in 50mL
121 of medium for preliminary enrichment culture.

122 **Culture media**

123 The culture media were both formulated on the basis of H3 medium (81 DSMZ) used for enrichment of
124 soil autotrophic bacteria. The medium consisted of 2.3g KH₂PO₄ and 2.9g Na₂HPO₄ 2H₂O per liter as buffer,
125 0.5g MgSO₄ 7H₂O, 0.01g CaCl₂ 2H₂O, 0.005g MnCl₂ 4H₂O, 0.005g NaVO₃ H₂O, and 5mL of SL-6 trace element
126 solution per liter of medium, with 5mL of vitamin solution. The SL-6 trace element solution consisted of
127 0.1g ZnSO₄ 7H₂O, 0.03g MnCl₂ 4H₂O, 0.3g H₃BO₃ 0.2 CoCl₂ 6H₂O, 0.01g CuCl₂ 2H₂O, 0.02g NiCl₂ 6H₂O, and
128 0.03g Na₂MoO₄ 2H₂O per liter of solution. The vitamine solution consisted of 10mg Riboflavin, 50mg
129 Thiamine-HCl 2H₂O, 50mg Nicotinic acid, 50mg Pyridoxine-HCl, 50mg Ca-Pantothenate, 0.1mg Biotin,
130 0.2mg Folic acid and 1mg Vitamin B₁₂ for 100 mL of distilled water. Iron citrate was added to the enrichment
131 bottles at a concentration of 0.05 g/L but not to the microbial bioelectrochemical systems in which the
132 cathode was used as sole electron source when only CO₂ was supplied. An organic carbon solution (organic
133 C) was composed of 2g/L D-glucose, 1g/L yeast extract, 1g/L Na-acetate, 1g/L DL-malic acid, 1g/L Na-
134 lactate, 1g/L Na-pyruvate, and 1g/L D-mannitol and used when indicated. NH₄Cl was added at 1 g/L only
135 when indicated. All enrichment procedures were maintained at 30°C and the pH was adjusted to 6.8 with
136 NaHCO₃ in the microbial bioelectrochemical systems and the enrichment cultures without organic C
137 addition. When the organic C solution was used, the pH was adjusted between 6.3 and 6.5.

138 **Design of microbial electrochemical system**

139 The electrochemical system used for our enrichment were composed of two chambers separated by
140 an anion exchange membrane (AEM) (fumasep® FAB-PK-130). The AEM was used to avoid the migration
141 of NH₄⁺ ions to the anodic chamber. Each chamber had a total volume of one liter. The pH of the reactors
142 was adjusted to 6.8 at the beginning of each batch experiment. Each system had a 25 cm² square carbon
143 felt working electrode with a thickness of 0.7 cm and a 16 cm² square Pt-Ir grid as a counter electrode. The
144 carbon felt electrodes were conditioned using chemical treatment with HCl, a flush with ethanol and a
145 heat treatment at +400°C as described elsewhere by Paul et al (Paul et al., 2018). The systems were
146 inoculated with the flask enrichments used for N₂ fixation in presence of organic C (N-free medium). After

147 inoculation, the organic C supply was reduced to 10% of the initial supply in all reactors. The organic C
148 supply was then totally replaced by CO₂ supply after 60 days. Two of the systems were polarized and two
149 other reactors were used as controls with open current voltage (non-polarized cathode enrichment, nPCE).
150 The working electrodes of the polarized cathode enrichment (PCE) were poised at a potential of -0.940 V
151 vs. saturated calomel electrode (SCE) used as a reference. The system was connected to a VMP3.0
152 potentiostat (BioLogic). The current was measured over time by a chronoamperometry method. The
153 current intensity was used to monitor the availability of electrons in the electroactive biofilm. An increase
154 of the current intensity was representative of an increase of the reduction reactions at the cathode. The
155 increase of these reduction reactions, abiotic or not, was assumed to bring more electrons to the bacterial
156 community. It was therefore assumed that an increase in current intensity was related to the enrichment
157 of bacteria able to use the cathode as electron source (Zaybak et al., 2013). The current density J was
158 calculated using the surface of the working electrode, i.e. 25 cm².

159 Before inoculation of the reactors, an initial chronoamperometry measurement was performed along
160 the first four days of operation with only organic carbon in the medium to determine the basal current
161 density in absence of bacteria. Two other abiotic reactors for 15 days were then implemented to measure
162 the current density in a medium without organic C. In order to validate the role of the cathode as electron
163 source, two OCV (nPCE) reactors were carried out. The current densities of the abiotics reactors over a
164 short period were therefore used as a reference to be compared with the measurements made after
165 inoculation and monitor the increase of the activity of reduction at the cathode.

166 Electrons required for the production of microbial metabolites and for biomass growth was then used
167 to calculate the Coulombic efficiency of the PCE according to the equations 1-5:

168
169 Eq. 1 $2.1 H_2 + CO_2 + 0.2NH_4^+ \rightarrow CH_{1.8}O_{0.5}N_{0.2} + 1.5H_2O + 0.2H^+$ for biomass production
170 (21 mol_e-/mol_{Nbiomass}) (Wresta et al., 2021)

171
172 Eq. 2 $N_2 + 3H_2 \rightarrow 2NH_3$ for nitrogen fixation (3 mol_e-/mol_{Nfixé}) (Zhang et al., 2022)

173
174 Eq. 3 $2CO_2 + 4H_2 \rightarrow CH_3COO^- + H^+ + 2H_2O$ for acetate production (8 mol_e-/mol_{CH₃COO}-)
175 (Wresta et al., 2021)

176
177 Eq. 4 $2H^+ + 2e^- \rightarrow H_2$ for H₂ production (2 mol_e-/mol_{H₂})

178
179 Eq. 5 $\eta_{CE} = \frac{n_e \times F \times n_{product}}{\int i dt}$

180 With η_{CE} the Coulombic efficiency in percentage of electron recovery in products, n_e moles of electrons
181 per moles of product (mol_e-/mol_{product}) calculated from the stoichiometric equations, F the Faraday
182 constant (96485 C.mol⁻¹), $n_{product}$ the number of mol_{product} and i the current intensity.

183 **Enrichment procedures**

184 Two enrichment procedures based on a sequential procedure by enriching separately N₂ fixation and
185 the use of an inorganic electron source were carried out. Each soil sample (Forest, Leguminous and
186 Compost) and a mix of all were used as inoculum in one batch of pre-enrichment. Pre-enrichment cultures
187 were then carried out in the same medium as first enrichment step for each procedure (i.e. supplied with
188 organic C for the first procedure and inorganic medium for the second) and for 20 days prior to be used as
189 inoculum in the enrichment procedures. Samples of the pre-enrichment were considered as initial
190 microbial community of the enrichments. Thus, at the end of pre-enrichment, the mixed culture was used
191 to inoculate two bottles of each enrichment and all unmixed soil samples were mixed to inoculate four
192 bottles of each enrichment.

193 The first enrichment cultures, polarized cathode and non-polarized cathode enrichments (PCE and
194 nPCE) were performed in three steps:

195 - The first step was performed in a 120 mL bottle with N-free medium supplemented with organic C
196 source. This first step was used to select N₂-fixing bacteria using organic compounds as electron donors.
197 The headspace was composed of an Ar/O₂/N₂ mixture (80/5/15) at 0.5 bar (absolute pressure). Cultures
198 were carried out in bottles containing 50 mL of liquid and 70 mL of headspace. Subcultures of these

199 enrichments were performed every 7 days for 6 weeks. The time between 2 subcultures was then reduced
200 to 3-4 days using 10% of the volume of the previous culture (5mL/50mL).

201 - After 55 days of enrichment in 10 successive batches, the N₂-fixing bacteria enriched cultures were
202 used to inoculate the cathodic chambers of the polarized microbial electrochemical system (Polarized
203 Cathode Enrichment, PCE) and the non-polarized microbial electrochemical system (non-Polarized Cathode
204 Enrichment nPCE). The same inorganic medium supplemented with 10% of the organic C source was fed
205 each week to start the enrichment of autotrophic bacteria. Inoculation of the cathode in presence of
206 organic C sources was made to favor bacterial growth. 80% of the medium was renewed every second
207 week to promote biofilm growth on the cathode. Headspace composition was monitored by GC and flushed
208 with N₂ if pO₂ exceeded 10% of the gas volume. Organic C supply was stopped when a significant current
209 density was measured in the polarized systems with regard to the controls.

210 - In the third and final enrichment step, CO₂ was used as sole carbon source as presented in Figure 1.
211 Organic C sources were then removed and the cathode was used as sole electron donor in reactor. Here,
212 only bacteria able to use cathode as electron source by direct interaction or indirect with H₂ were able to
213 grow. A 80/20 (v:v) CO₂/N₂ atmosphere was set up in the headspace with trace amounts of O₂ (< 5%). The
214 medium was replaced every 15-30 days. The gas recycling vessel was filled with CO₂ and was replaced with
215 a new one when O₂ exceeded 5% of the volume due to gas volume depletion. The nPCE controls were
216 operated in the same conditions as the polarized systems but without monitoring the current density. The
217 only available electron source in the nPCE controls was the organic C fed at the beginning of the
218 enrichment.

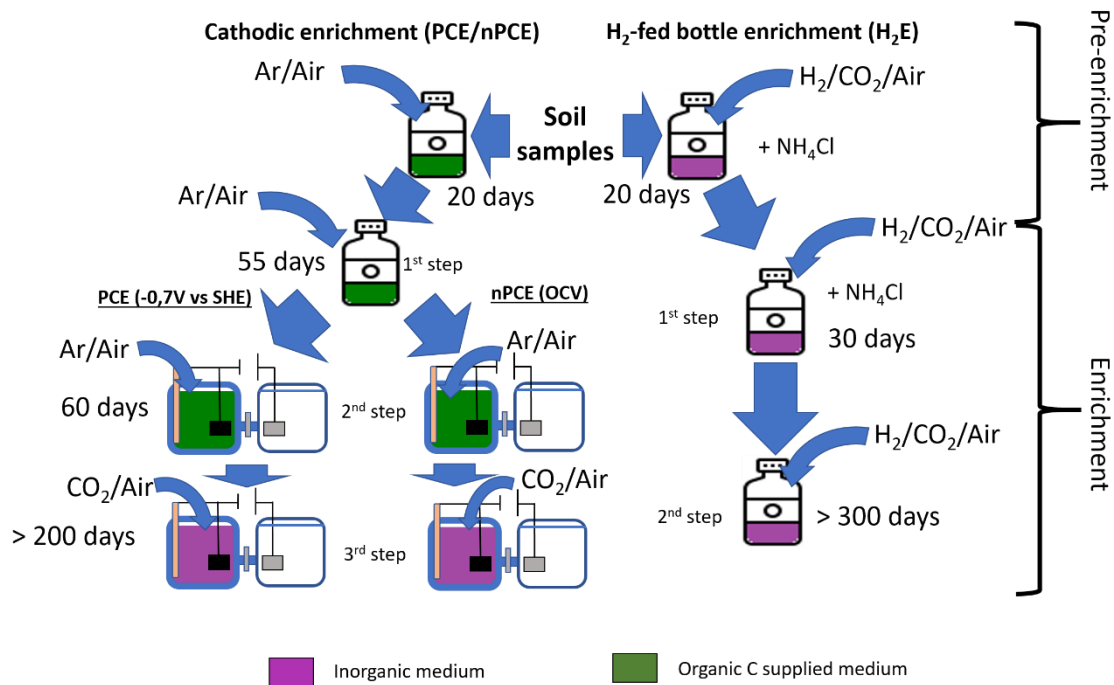
219 In the second enrichment method, the H₂-fed enrichment (H₂E), autotrophic bacteria were enriched in
220 inorganic medium supplemented with H₂ as sole electron source. These enrichments on H₂ were obtained
221 by pre-enriching in strict autotrophic bacteria using 50 ml of inorganic medium in a 120 ml bottle. The
222 headspace consisted of a mixture of 75/15/8/2 (v:v:v:v) H₂/CO₂/N₂/O₂ at an initial pressure of 1.5 bar
223 (absolute). Two two-weeks batches (30 days) were performed with NH₄Cl (1g/L) as nitrogen source in the
224 first stage of this enrichment as seen in Figure 1. This nitrogen source was then replaced by N₂ as only N
225 source to enrich N₂-fixing bacteria in the second stage of enrichment. Centrifugation (10min, 7500 RPM,
226 ~7500g) of 80% of the initial medium (40mL) was done at each subculture every 15-20 days. The pellets
227 obtained after centrifugation were suspended in 5mL of sterile medium before being used for subculturing.
228 Table 1 presents a summary of the different procedures used.

229 **Table 1** - Comparison between each enrichments procedure used in this work.

	PCE	nPCE	H ₂ E
Enrichment reactor	Bottle then cathodic chamber	Bottle then cathodic chamber	Bottle
Electrode	Yes	Yes	No
Applied potential	-0,7 V vs SHE	Open circuit voltage	NA
Enrichment step	3 steps (1) soil diazotrophic bacteria in bottle (2) diazotrophic bacteria in MEC (3) autotrophic diazotrophic bacteria in MEC	3 steps (1) soil diazotrophic bacteria in bottle (2) diazotrophic bacteria in MEC in OCV (3) control without electron sources	2 steps (1) soil autotrophic bacteria in bottle (2) autotrophic diazotrophic bacteria in bottle
Number of Batch	(1) 10 (2) 4 medium replacement (3) 14	(1) 10 (2) 4 medium replacement (3) 14	(1) 2 (2) 25
Batch duration	3-7 days (Organic C) 15-30 days (CO ₂)	3-7 days (Organic C) 15-30 days (CO ₂)	15-30 days
Enrichment duration	>300 days	> 300 days	> 300 days
Electron donor	(1) (2) Organic C (2) (3) Cathode (direct or indirect)	(1) (2) Organic C (3) none	(1) NH ₄ Cl and H ₂ (2) H ₂
Electron acceptor	O ₂ /N ₂ /CO ₂	O ₂ /N ₂ /CO ₂	O ₂ /N ₂ /CO ₂

230

231



232

233

Figure 1 - Diagram of the enrichment process

234 Medium analyses

235 NH₄⁺, NO₂⁻ and NO₃⁻ concentrations were measured using a Gallery+ sequential analyzer (Thermo Fisher
 236 Scientific). Two mL of samples were centrifuged at 13500 RPM (~12300g) and then filtered to 0.2µm with
 237 nylon membranes before being stored at 4°C. The remaining pellets were stored at -20°C and used for
 238 community analysis. VFAs and other carbon compounds were measured on Clarus 580 GC equipped with
 239 FID and a Dionex UltiMate 3000 HPLC as described elsewhere (Carmona-Martínez et al., 2015; Moscoviz et
 240 al., 2019)

241 Total nitrogen was measured using a CHNS Flashsmart elemental analyzer (Thermo Fisher Scientific).
 242 The sample (approximately 2.5 mg) was weighed and was introduced into the oxidation/reduction
 243 chamber of the analyzer. 200 mL of medium were sampled at each medium change. These samples were
 244 dried for 4-5 days at 60°C. The samples were then freeze-dried and then grounded with a mortar. Two to
 245 four mg of each sample was used in the CHNS analyzer. The nitrogen content was then compared to the
 246 dry weight measured before freeze-drying to determine the mass of nitrogen in the medium. No CHNS
 247 analysis was performed on H₂-based enrichment due to a low culture volume (50mL).

248 Nitrogen present in the biomass (biofilm and planktonic) was estimated from quantification of 16S
 249 rDNA with qPCR. The rrnDB-5.7 database was used to estimate the actual bacterial amount from 16S rDNA
 250 qPCR using theoretical 16S rDNA copies/genome per strain, genus or family given by the database and
 251 sequencing results from our communities (Stoddard et al., 2015). Then, the theoretical calculated number
 252 of bacteria was used to determine the nitrogen content in the biomass using the theoretical average dry
 253 mass of an *Escherichia coli* cell of 216×10⁻¹⁵ g/bacterium and with a theoretical relative mass of nitrogen in
 254 microbial biomass, ie. 11.4% according to the average biomass formula CH_{1.8}O_{0.5}N_{0.2} (Heldal et al., 1985;
 255 Loferer-Krößbacher et al., 1998). The nitrogen present in the biomass was therefore estimated using the
 256 formula below:

257

$$258 \text{ Eq. 6 } N_{(in\ biomass)} = \text{theoretical bacteria count} \times \text{mass } E. coli \times \text{relative mass of } N \text{ in biomass}$$

259

260 With $N_{in\ biomass}$ the nitrogen concentration in the medium from biomass in mg_N/L, the *theoretical*
 261 *bacteria count* based on the calcul of concentration in bacteria with results of qPCR of 16S rDNA for each
 262 enrichment (number of bacteria/L), *mass E. coli* a constant of 2.16 10⁻¹⁰ mg/cell_{E. coli} and *relative mass of N*
 263 *in bacteria* is 11.4% of the dry mass.

264 Gas analysis and acetylene reduction assay (ARA)

265 CO₂, H₂ and N₂ used in the headspace of the enrichments were provided at laboratory grade. Pure
266 ethylene was also supplied for calibration of the gas chromatography ethylene measurement.

267 Headspace compositions and pressures were analyzed every 1-2 days. The pressure was manually
268 measured with a Keller LEO 2 manometer (KELLER AG, Wintherthur, Switzerland). Gas analyses were
269 carried out on a Perkin Elmer Clarus 580 GC equipped with RT-Q-Bond and RT-MSieve 5Å columns with a
270 TCD allowing the quantification of H₂, CO₂, N₂, O₂ and CH₄ with Ar as carrier gas as described by A. Carmona-
271 Martínez (Carmona-Martínez et al., 2015). Acetylene and ethylene were measured using a Perkin Elmer
272 Clarus 480 GC equipped with RT-U-Bond and RT-MSieve 5Å columns with TCD and He as carrier gas as
273 described in a previous work (Carmona-Martínez et al., 2015).

274 The acetylene reduction assay (ARA) was performed to quantify the rate of N₂ fixation using the ability
275 of nitrogenases to reduce acetylene to ethylene. This reaction occurs at a rate proportional to the rate of
276 N₂ fixation according to the theoretical ratio C₂H₂:N₂ (3:1) (Bergersen, 1970). The ARA was performed only
277 after 18 batch cycles for H₂-fed enrichment (H₂E) and 11 batch cycles in polarized cathode enrichment (PCE)
278 fed with CO₂ (340 days). Acetylene concentration were calculated as follow :

$$279 \text{ Eq. 7 } n_{C_2H_4} = \frac{P_{NaOH}V_{C_2H_4}}{RT} = \frac{(P_{total} - P_{CO_2}) \times V \times \%_{C_2H_4}}{RT}$$

280 With (P_{total} the pressure in headspace, P_{CO_2} the partial pressure of CO₂ measured without CO₂ trap, V
281 the volume of gas in headspace, $\%_{C_2H_4}$ the part of C₂H₄ measured by GC-TCD in headspace, R the perfect
282 gas constant and T , the temperature of the reactor.

283 And Acetylene production rate were calculated following next equation:

$$284 \text{ Eq. 8 } \Delta[C_2H_4] = \frac{[C_2H_4]_{t1} - [C_2H_4]_{t0}}{t1 - t0} = \frac{\frac{n_{C_2H_4,t1}}{V} - \frac{n_{C_2H_4,t0}}{V}}{t1 - t0}$$

285 With $\Delta[C_2H_4]$ the rate of C₂H₄ production in $\mu\text{mol/L.d}$, $t0$ the last measure without C₂H₄ observed,
286 $t1$ the first measure of C₂H₄ in headspace and V the volume of liquid which is constant between two ARA
287 measurement.

288 A specific N₂-fixing activity was then calculated with the N₂-fixing bacteria measured by quantification
289 of the *nifH* gene used as a marker for these bacteria. This specific activity corresponds to the rate of C₂H₄
290 produced per bacteria capable of fix N₂ measured by qPCR of *nifH* gene. The acetylene used for the
291 acetylene reduction assay (ARA) was obtained by adding calcium carbide (CaC₂) in water and recovered in
292 a bag. The acetylene concentration in the bag was then measured by gas chromatography. Gas from the
293 bag was added to each enrichment to reach a composition of 10% V/V acetylene and an equivalent amount
294 of gas was removed from the headspaces. Ethylene production was then daily monitored for 7 days in the
295 microbial electrolysis systems (PCE and nPCE) and 15 in the H₂E bottles by the Perkin Elmer Clarus 480 GC
296 with TCD. To ensure separation of ethylene from CO₂ on the RT-U-Bond column, a CO₂ trap with sodium
297 hydroxide (6M NaOH) was used at the time of sampling and is taken into account in the calculations. After
298 the ARA method was completed, the headspaces were flushed with N₂ and the gas recycling system was
299 changed.

300 Community sequencing and biomass quantification

301 The microbial communities were quantified using the 16S rDNA qPCR to determine the total bacterial
302 concentration and *nifH* gene qPCR for N₂-fixing bacteria. In parallel, 16S rDNA sequencing was performed
303 to identify major members of each community. This sequencing was also necessary to convert the amount
304 of 16S rDNA to total bacteria using the rrnDB-5.7 database. To analyze the communities present in
305 suspension, 1.8 mL of sample were collected for qPCR. For the cathodes, 1 cm² was recovered at several
306 times. The piece of carbon felt was then chopped with a sterile scalpel before being immersed in 20 mL of
307 sterile inorganic media. 1.8 mL was then recovered after shaking 20 mL of medium to resuspend as much
308 biomass as possible. These samples were then centrifuged 10 min 13500 RPM (12340g). The supernatant
309 was discarded and the pellets retained for DNA extractions. After qPCR, the concentrations measured in
310 the electrode samples were expressed considering the volume of medium.

311 Genomic DNA was extracted using the PowerSoil™ DNA Isolation Sampling Kit (MoBio Laboratories,
312 Inc., Carlsbad, CA, USA) according to the manufacturer's instructions. The qPCR amplification program was
313 performed in a BioRad CFX96 Real-Time Systems C1000 Touch thermal cycler (Bio-Rad Laboratories, USA).
314 For the analysis of total bacteria, primers 330F (ACGGTCCAGACTCCTACGGG) and 500R
315 (TTACCGCGGCTGCTGGCAC) were used. For the bacteria qPCR mix: SsoAdvanced™ Universal SYBR Green
316 Supermix (Bio-rad Laboratories, USA), primer 330F (200 nM), primer 500R (200 nM), 2 µL of DNA, and
317 water were used to a volume of 12 µL. The qPCR cycle was as follows: incubation for 2 min at 95°C and 40
318 cycles of dissociation (95°C, 10 s) and elongation (61°C, 20 s) steps. The results were then compared to a
319 standard curve to obtain the copy number of the target in the sample. Both the 16S rDNA concentration
320 of the PCE media and the cathodes are considered in the calculation of the total 16S rDNA concentration
321 of the PCE. These concentrations are used as an indicator of the biomass present and the use of a database
322 of the number of 16S operons per bacterial genome was used to estimate the actual amount of bacteria.

323 The presence of N₂-fixing bacteria was monitored by qPCR of the *nifH* gene of the Fe-Fe subunit of
324 nitrogenases (Dos Santos et al., 2012; Gaby & Buckley, 2012). The *nifH* gene is known as marker of N₂ fixing
325 bacteria, common to all nitrogenases and is used for their quantification because of its necessary presence
326 for the fixation of N₂ (Dos Santos et al., 2012; Gaby & Buckley, 2012). All qPCR amplification programs were
327 performed in a BioRad CFX96 Real-Time Systems C1000 Touch thermal cycler (Bio-Rad Laboratories, USA).
328 The primers PolF-TGCGAYCCSAARGCBGACTC and PolRmodify reverse-AGSGCCATCATYTCRCCGGA were
329 used (Poly et al., 2001). The mixture: 6µl SsoAdvanced™ Universal SYBR Green Supermix (Bio-rad
330 Laboratories, USA), F primer (500 nM), R primer (500 nM), 2 µL of DNA and water was used up to a volume
331 of 12 µL. The qPCR cycle was as follows: incubation for 2 min at 95°C and 40 cycles of dissociation (95°C,
332 30 s) and elongation (60°C, 30 s) steps. Then, the results were compared to a standard curve to obtain the
333 number of copies of the target in the sample. These two quantifications allow us to calculate the ratios of
334 N₂-fixing bacteria per total bacteria of the enrichments at different points to track the enrichment of N₂-
335 fixing bacteria. This ratio can also help us to derive hypotheses on the functioning of our communities that
336 can be completed by the analysis of the communities during sequencing.

337 After quantification, our enriched communities were sequenced according to their 16S rDNA and the
338 results are available on NCBI repository PRJNA976100, Biosample SAMN28447998-SAMN28448066. The
339 V3-V4 region of the 16S rDNA was amplified using universal primers as reported elsewhere (Carmona-
340 Martínez et al., 2015). The PCR mixture consisted of MTP Taq DNA Polymerase (Sigma-Aldrich, Germany)
341 (0.05 u/µL) with enzyme buffer, forward and reverse primers (0.5 mM), dNTPs (0.2 mM), sample DNA (5-
342 10 ng/µL), and water to a final volume of 60 µL. 30 cycles of denaturation (95°C, 1 min), annealing (65°C, 1
343 min), and elongation (72°C, 1 min) were performed in a Mastercycler thermal cycler (Eppendorf, Germany).
344 A final extension step was added for 10 min at 72 °C at the end of the 30th amplification cycle. PCR
345 amplifications were verified by the 2100 Bioanalyzer (Agilent, USA). The GenoToul platform (Toulouse,
346 France <http://www.genotoul.fr>) used an Illumina Miseq sequencer (2 x 340 bp pair-end run) for the
347 sequencing reaction. The raw sequences obtained were analyzed using bioinformatic tools. Mothur version
348 1.39.5 was used for cleaning, assembly and quality control of the reads. Alignment was performed with
349 SILVA version 128 (the latter was also used as a taxonomic contour).

350 Communities sequenced on pre-enrichment bottles were used as initial community of the enrichment
351 cultures. For PCE and nPCE, sequenced communities came from the biofilm formed on electrodes. Two
352 replicates per potential were used. For H₂E bottles, 6 bottles were used for sequence analysis and qPCR.
353 For pre-enrichment, sequences corresponded to each soil samples (leguminous, forest, compost) and a
354 mix of them.

355 **Data analysis**

356 All results were analyzed using R (4.2.0) and Rstudio (2022.07.1) for calculations and graphics. The
357 Tidyverse package was used for data manipulation (*Tidyverse*, n.d.). The packages ggplot2, ggpubr, scales,
358 cowplot, corrplot and palettetown were used for the graphical representations. Visual representation of
359 bacterial relative abundances was performed with the phyloseq package (McMurdie, 2011/2023). Inkscape
360 software was also used to edit the graphs when necessary. The uncertainties shown for the values
361 presented are standard deviations. All data and scripts used here are available online (Rous, 2023).

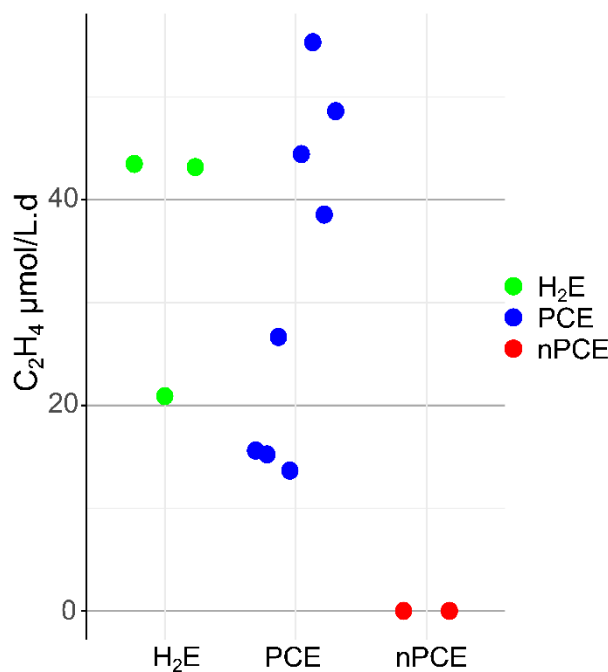
362

363

Results and discussion

364 Nitrogen fixation after 340 days of enrichment

365 N_2 fixation was quantified at the day 340 of the enrichment using acetylene reduction assays (ARA).
366 This assay was performed in H_2 -fed bottle enrichments (named 'H₂E'), in polarized cathode enrichment
367 (named 'PCE') and in the non-polarized cathode enrichments as controls (named 'nPCE'). As shown in
368 Figure 2, the ARA results confirmed the N_2 fixation capacity of the enriched communities (Bergersen, 1970).
369 This indicates that the cathode and/or H_2 was used as electron sources for N_2 fixation both in PCE and in
370 H₂E bottles. The average rates were similar in both enrichment methods with $32 \pm 17 \mu\text{molC}_2\text{H}_4/\text{L.d}$ in PCE
371 and $36 \pm 13 \mu\text{molC}_2\text{H}_4/\text{L.d}$ in H₂E bottles. The PCE corresponding N_2 fixation rates ranged from 0.12
372 $\text{mg}_{\text{Nfixed}}/\text{L.d}$ (minimum) to 0.51 $\text{mg}_{\text{Nfixed}}/\text{L.d}$ (maximum), which is consistent with the rate of 0.2 $\text{mg}_{\text{Nfixed}}/\text{L.d}$
373 estimated by Rago et al. (2019) and also with N_2 fixation rates reported for soil bacteria (Hardy et al., 1973;
374 Kifle & Laing, 2016; Rago et al., 2019). Despite these significant N_2 fixation rates and the long duration of
375 the experiments, the rate of ammonium production in solution remained lower than 0.07 $\text{mg}_N/\text{L.d}$ at the
376 day 340 (Table 2), indicating that most of the fixed N_2 was probably rapidly used by bacteria.
377



378

379 **Figure 2** - Reduction rate of acetylene in $\mu\text{mol C}_2\text{H}_4/\text{L.d}$ in the different reactors after 340 days of operation . or H_2
380 condition, 3 bottles were used for the acetylene reduction assay with one injection for each bottle, i.e. 3 measurements.
381 For PCE, 2 reactors were used and 4 injections were made to validate the repeatability of the measurement when C_2H_4
382 which gives 8 measurements for each of these two conditions. For nPCE, 2 reactors were used which gives 2
383 measurements for each conditions.

384 The ability of the microbial communities to fix N_2 was also assessed by qPCR of the *nifH* gene (Dos
385 Santos et al., 2012; Pogoreutz et al., 2017). The amounts of N_2 -fixing bacteria after 340 days of enrichment
386 are reported in Table 2. The average *nifH* gene concentration in PCE was estimated at $7.8 \cdot 10^7$ copies_{*nifH*}/mL,
387 two orders of magnitude higher than the average concentration of $8.3 \cdot 10^5$ copies_{*nifH*}/mL measured in the
388 H₂E enrichment bottles. This observation was surprising since N_2 -fixation rates were similar in both
389 configurations (Figure 2). This suggests that the fixation rate per *nifH* copy was much higher in H₂E than in
390 PCE. The estimated specific activities per *nifH* copy were indeed of $0.2 \pm 0.3 \mu\text{molC}_2\text{H}_4/10^8$ copies_{*nifH*}.d in the
391 PCE and $2.1 \pm 0.7 \mu\text{molC}_2\text{H}_4/10^8$ copies_{*nifH*}.d in H₂E bottles (Table 2). Furthermore, the comparison between
392 *nifH* gene and 16S rDNA copy numbers gives an idea of the proportions of N_2 fixing bacteria in each
393 microbial community. Interestingly, this proportion was 18% in H₂E bottles that was four times higher than
394 the value of 4.6% in PCE (Table 2). Therefore, N_2 -fixing bacteria constituted a smaller proportion of the

395 bacterial populations in PCE than in H₂E and only a small proportion of the bacteria participated to N₂
396 fixation in the PCE. In nPCE controls, the biomass was higher than in H₂E and the *nifH*/16S ratio lower (Table
397 2). This higher biomass concentration was likely due to the enrichment period in presence of organic C (day
398 0 to 115 including 60 days in BES) for the PCE and nPCE enrichments. NH₄⁺ in nPCE was also observed at a
399 rate of 0.07 mg/L.d as presented in Table 2 but without acetylene accumulation, meaning that no N₂
400 fixation occurred. In absence of electron source, nPCE enrichment communities could have been
401 maintained through cryptic growth. The presence of NH₄⁺ in the nPCE was likely related to cell lysis since
402 no measurable fixation was detected by ARA even though significant biomass production was observed.

403 **Table 2** - The average ammonium production rates, the number of *nifH* gene copies, the number of 16S gene copies,
404 and the *nifH*/16S ratio were assessed after 340 days for the three experimental configurations. Average values were
405 measured on the last batch of 21 days, before 340 days of enrichment for the two polarized cathode enrichment (PCE), the
406 two non-polarized Cathode Enrichments (nPCE) and the six H₂ enrichment bottles (H₂E)

	PCE	nPCE	H ₂ E
N-NH ₄ ⁺ mg/L.d	0.07±0.01	0.07±0.01	0.04±0.03
<i>nifH</i> gene copies /mL	7.8±9.5 10 ⁷	2.5±2.8 10 ⁶	8.3±2.2 10 ⁵
16S rDNA gene copies /mL	1.7±1.9 10 ⁹	1.4±0.2 10 ⁸	4.6±1.5 10 ⁶
<i>nifH</i> /16S	3.8 %	1.7 %	19.0 %

407

408 **Current density and Autotrophic enrichment in polarized cathode enrichment**

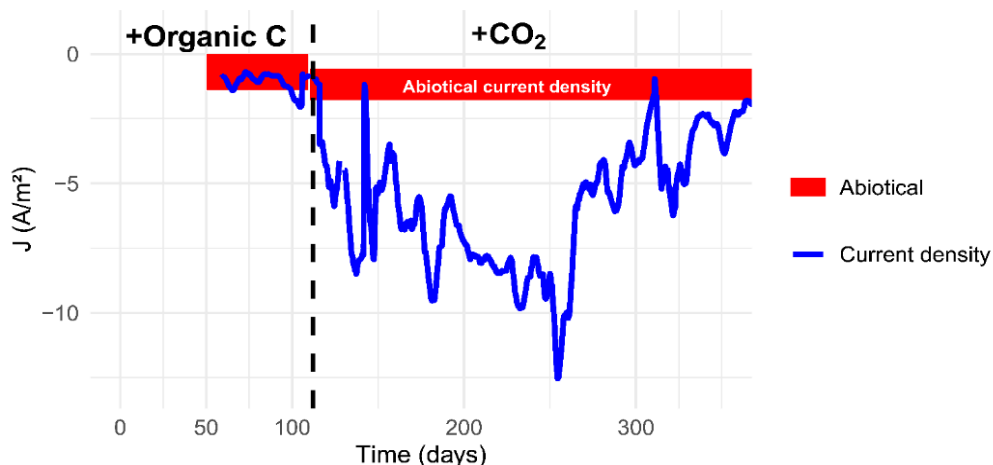
409 The average current density for the two PCE over experimental time is shown in Figure 3. As the current
410 measured at the cathode was negative by convention, a more negative corresponded to a higher reduction
411 activity. Regarding the current densities in the abiotic systems, the average current densities were
412 measured at -0.75 A/m² for two times four days with an organic C source and -1.1 A/m² for 16 days with
413 only CO₂ as the carbon source.

414 The average current density measured in the PCE was not different from the current density measured
415 in the abiotic control (approximately -1 A/m² with organic C supply) for the first 45 days of operation (days
416 55 to 100 of the enrichment). An increase up to -2 A/m² appeared between 100 and 115 days of enrichment
417 in PCE. CO₂ was then used as sole carbon source after this increase appeared. Following this change in
418 carbon source, a sharp increase in current density to -5 A/m² was observed in the PCE with regards to the
419 range of current densities in the abiotic controls (approximately -2 A/m² on CO₂)(Figure 3). The higher
420 current density was assumed to be associated to the electroactive activity of electron uptake by enriched
421 bacteria. The current density in the PCE then continuously increased until day 250 of the enrichment to
422 reach a value of -15 A/m².

423 The high current density observed after 250 days of enrichment indicated a high redox activity linked
424 either to hydrogen evolution, oxygen reduction, or possibly direct electron transfer. As proposed by Z.
425 Zaybak et al. (2013), the high activity was probably resulting from a high metabolic activity in the biofilm
426 with significant microbial catabolic process (Zaybak et al., 2013). Compared to the current densities
427 obtained Rago et al. (2019) in the order of magnitude of -10 mA/m² at the same potential (-0.7 vs SHE), the
428 current densities observed here (-5 to -10 A/m²) were about 1000 times higher. These current density levels
429 are close to those measured by Zhang et al. (2022) who reported a maximum of -10 A/m² at the same
430 applied potential (Zhang et al., 2022).

431 After 230 days, power failures occurred, interrupting temporarily the current supply to the cathodes.
432 An important decrease of the current density was observed afterwards, down to -5 A/m² after 260 days
433 and -3 A/m² after 320 days. The lower current density reflected a change in the functioning of the microbial
434 communities, leading to less electron exchange with the cathode.

435



436

437 **Figure 3** - Mean current density measured for the two PCE (blue line). Levels shown in red correspond to theoretical
438 mean current density and standard deviation estimated from two abiotic electrochemical systems current densities. For
439 abiotic electrochemical system, one batch of 2 days were made with Organic C and one batch of 16 days with CO₂. The
440 peaks observed are due to the batch operation of the PCE with disturbances each time the medium was renewed. Power
441 failures occurred at 230 days and 260 days. The time indicated on the x axis corresponds to the experimental time starting
442 at day 0 of the enrichment where soil samples were first introduced in the bottles with a medium containing organic C. Day
443 55 corresponds to the start of microbial electrochemical system with the precultured communities. The dashed line on day
444 110 corresponds to the passage on CO₂ as the sole carbon source in PCE. A 5-day curve smoothing was applied on PCE
445 current density curve.

446 **Biomass quantification**

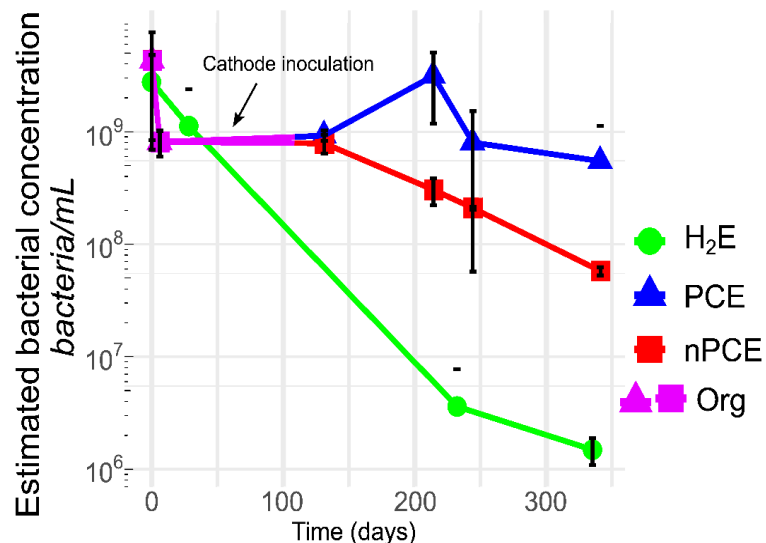
447 Bacterial biomass was monitored in the enrichments by measuring 16S rDNA concentrations by qPCR
448 (Figure 4). At day 131 (18 days after switching from organic C to CO₂), the average 16S rDNA concentrations
449 measured in the polarized cathode enrichment (PCE) and in the non-polarized cathode enrichment (nPCE)
450 controls were $4.6 \pm 0.4 \cdot 10^9$ and $4.2 \pm 1.2 \cdot 10^9$ copies 16SrDNA/mL, respectively. These concentrations
451 corresponded to $9.4 \pm 1.0 \cdot 10^8$ and $8.0 \pm 1.5 \cdot 10^8$ bacteria/mL, respectively, as presented in Figure 4. These
452 bacteria concentrations resulted from the first enrichment phase with organic C. During this phase, organic
453 substrates were used as carbon and electron sources for biomass growth in both configurations (PCE and
454 nPCE). At day 214, the 16S rDNA concentration in the PCE was used to calculate a concentration of 3.3 ± 2.1
455 $\cdot 10^9$ bacteria/mL, corresponding to a biomass increase by a factor of 3.5 between 131 and 214 days (Figure
456 4). At the same time, the bacterial concentration dropped in nPCE from $8.0 \pm 1.5 \cdot 10^8$ bacteria/mL to 3.0 ± 0.8
457 $\cdot 10^8$ bacteria/mL. This drop was explained by the lack of available energy source for growth, which led to a
458 sharp decrease of the bacterial populations. At day 214, the 16S rDNA concentration in PCE was therefore
459 11-fold higher than in nPCE controls. This difference is consistent with the difference reported by Rago *et*
460 *al.* between polarized and non-polarized conditions, with electroactive biocathodes enriched in
461 autotrophic diazotrophic bacteria (Rago *et al.*, 2019). These results suggested that the enriched microbial
462 communities were able to use the electrodes polarized at -0.7 V vs. SHE as sole electron sources to grow
463 while fixing N₂.

464 In the H₂-fed enrichment (H₂E) bottles, the 16S rDNA concentration steadily decreased along the
465 experiment. The concentration decreased from $1.1 \pm 1.3 \cdot 10^9$ bacteria/ml at the beginning of the enrichment
466 down to $1.3 \pm 0.3 \cdot 10^6$ bacteria/ml after 340 days (Figure 4). These concentrations appear lower than the
467 biomass concentrations observed in the PCE medium at the same time of enrichment, i.e. $4.5 \pm 5.9 \cdot 10^6$
468 bacteria/mL at day 244 and $8.6 \pm 8.8 \cdot 10^6$ bacteria/mL at day 340. These results confirm that bacterial growth
469 was higher on the cathodes than in an H₂ supplied environment. It was therefore concluded that the PCE
470 provided more favorable environment for biomass growth than H₂ fed bottles as the surface provided by
471 the electrode was likely favorable for biofilm growth.

472 We also calculated the *nifH*/16S ratio representing the part of bacteria able to fix N₂ among the total
473 bacteria. A ratio of 0.0006 of *nifH* gene copies per 16S rDNA copy was measured for samples at the very
474 beginning of enrichment, both for H₂E and PCE. After 131 days, corresponding to the switch to CO₂ as sole
475 C-source, this level increased to 0.03 in PCE and 0.02 in nPCE control. These results are consistent with an

476 enrichment in diazotrophic bacteria during the enrichment phase on organic carbon (Bowers et al., 2008).
477 The bacterial enrichment in nPCE was likely possible as the organic C was used by the bacteria as energy
478 source. After 214 days, the level decreased to 0.02 in PCE but remained higher than the level at the
479 beginning of enrichment. This variation suggests interactions within the community that favored the
480 growth of non-N₂ fixing bacteria after the shift to CO₂ as sole C-source. After 340 days, the ratio of *nifH* to
481 16S rDNA was 0.04 as presented in Table 2. In parallel, a ratio of *nifH* to 16S rDNA of 0.90 was measured for
482 H₂E at 244 days. Therefore, most of the bacteria were able to fix N₂ in H₂E bottles, confirming the efficient
483 enrichment in diazotrophic bacteria (Bowers et al., 2008). Given the loss of biomass observed in H₂E during
484 the experiment (Figure 4), this high ratio corresponded likely to the surviving bacteria that were selected
485 on their ability to fix N₂. The ratio measured in these H₂E then decreased down to 0.19, suggesting a
486 decrease in N₂-fixing bacteria in biomass.

487 As previously mentioned, after 230 days, power failures occurred and interrupted the polarization of
488 the electrodes. These interruptions impacted the microbial communities with a decrease in biomass
489 concentration to $8.1 \pm 7.6 \cdot 10^8$ bacteria/mL at 244 days and $5.5 \pm 6.0 \cdot 10^8$ bacteria/mL after 340 days compared
490 to the concentration of $3.3 \cdot 10^9$ bacteria/mL measured at 214 days. At the same time, the *nifH*/16S rDNA
491 ratio increased up to 5%, indicating that N₂-fixing bacteria were more resistant. Nevertheless, a decrease
492 was observed in *nifH* quantities, from $2.3 \cdot 10^8$ copies_{*nifH*}/mL after 214 days to $7.8 \cdot 10^7$ copies_{*nifH*}/mL after 340
493 days.
494



495

496 **Figure 4** - Bacteria concentrations over time in the different enrichments calculated from 16S rDNA qPCR
497 quantifications in bulk and biofilm. Green disks correspond to H₂ enrichments in bottles, blue triangles correspond to
498 polarized cathode enrichment (PCE), red squares correspond to controls in non-polarized cathode enrichment (nPCE). The
499 partially purple symbols marked Org correspond to the first phases of enrichment with organic C for the PCE and nPCE. The
500 arrow indicates the transition from bottle enrichments to cathode enrichments in microbial electrochemical systems for
501 PCE and nPCE. Error bars correspond to the calculated standard deviation.

502 N quantification and coulombic efficiency

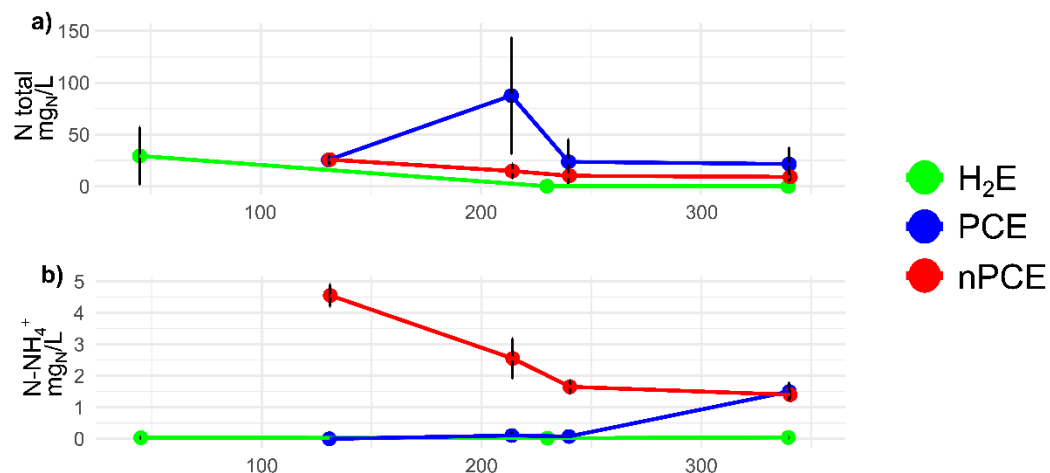
503 Total N contents of the different experiments are shown in Figure 5a. The total N corresponded to the
504 sum of the nitrogen measured in the liquid phase by N-ion concentration analysis (N-NH₄⁺, N-NO₃⁻, N-NO₂⁻
505), in the medium by CHNS elemental analysis for PCE and nPCE, in the suspended biomass from qPCR results
506 only for H₂E where the dry mass was not measured, and on the electrode based on the bacterial
507 concentrations. The total N concentration was estimated after 131 days of enrichment (ie. before the shift
508 to CO₂ as sole C source) at 25.5 ± 0.4 mg_N/L and 25.8 ± 4.7 mg_N/L in the PCE and in the nPCE controls,
509 respectively. After 214 days of enrichment, total N increased up to 87.6 ± 56.1 mg_N/L in the PCE with regards
510 to the low value of 14.8 ± 7.0 mg_N/L in the nPCE controls. Ammonium represented only a small fraction of
511 the total N in the PCE. The maximum ammonium concentration observed at a batch end in the PCE was
512 1.5 ± 0.3 mg_N/L at the day 340 of the enrichment in comparison with the maximum value of 4.5 ± 0.4 mg_N/L
513 found in nPCE control after 131 days (1.4 mg_N/L at the day 340)(Figure 5b). The average N fraction in the

514 form of ammonium was therefore of 12% in nPCE and only 1.6% in PCE. It was thus assumed that the higher
515 level of ammonium in nPCE was related to the decay of biomass in absence of electron sources. In
516 counterpart, the ammonium produced by N_2 fixation in the PCE was likely directly used for protein
517 synthesis as suggested elsewhere (Bueno Batista & Dixon, 2019; Temple et al., 1998). In addition, nPCE $N-$
518 NO_3^- concentrations were 5 to 15 times lower than $N-NH_4^+$ concentrations with maximum values of 0.9
519 mg_N/L $N-NO_3^-$ in the nPCE control and 0.2 mg_N/L $N-NO_3^-$ in PCE. An average concentration of 0.1 ± 0.2 mg_N/L
520 $N-NO_3^-$ in H₂E bottles was also observed. NO_2^- concentrations were negligible.

521 Using our method of N mass estimation on biomass lost as presented in Figure 4 for nPCE, the total
522 concentration of N lost by biomass would be estimated around 130 to 200 mg_N/L depending on the
523 community (2 nPCE). This loss would then be equivalent to rates of 0.6 to 0.9 $mg_N/L.d$ released by this the
524 biomass on average along the enrichment. Assuming a loss of a constant portion of biomass, a release rate
525 of 0.1 $mg_N/L.d$ was estimated as average for the batch ending at 340 days, close to the 0.07 $mg/L.d$
526 presented in Table 2. This result supported our hypothesis that NH_4^+ release was linked to biomass loss in
527 nPCE enrichments after organic C addition was stopped.

528 The H₂ enrichment bottles (H₂E) showed an average $N-NH_4^+$ accumulation of 35.6 ± 36 $\mu g_N/L$ after 131
529 days and an average of 0.1 ± 0.2 mg_N/L over the duration of enrichment. This concentration represented a
530 small fraction of the total N at the very beginning of the enrichment, with an estimated concentration of
531 29.4 ± 28 mg_N/L . The N concentration decreased during the enrichment, which is consistent with the
532 biomass loss as shown in Figure 4. H₂E were therefore less efficient for N_2 accumulation than polarized
533 cathode enrichment, with a lower microbial biomass production.

534



535

536 **Figure 5** - (a) Total N concentration based on the sum of (1) N estimated from biomass measurement (suspended
537 biomass and biofilm), (2) N content in ionic forms ($N-NH_4^+$, $N-NO_3^-$, $N-NO_2^-$) and (3) N measured in the dry weight of the
538 medium of the polarized cathode enrichment (PCE) and non-polarized cathode enrichment (nPCE) and (b) $N-NH_4^+$
539 concentration in H₂ enrichment (H₂E), PCE and nPCE.

540 Current densities and rates of acetate production, N_2 fixation and biomass growth are shown in Table
541 3. Coulombic efficiencies associated with each reaction were estimated based on these results (Table 3).
542 During the first 214 days of enrichment, 0.6 to 3.3% of the electrons were used for N_2 fixation in the two
543 PCE. In comparison, efficiencies of 0.5% and 20% for NH_4^+ synthesis was reported in two recent works
544 carried out under similar conditions (Yadav et al., 2022; Zhang et al., 2022). As the amount of fixed N was
545 highly dependent on biomass accumulation, negative results were obtained at day 244 when biomass
546 started to decrease. The electrons used at the cathode for biomass synthesis during the first period (131
547 to 214 days) accounted for 2.8% and 17.3% in the two PCE. These high coulombic efficiencies were probably
548 also associated to acetotrophic and acetogenic bacteria. Indeed, acetate produced using electron from the
549 cathode could have been used by acetotrophic bacteria for growth, lowering coulombic efficiency of
550 acetogenesis and increasing CE for bacterial growth. As acetogenic bacteria do not tolerate the presence

551 of oxygen, dissolved O₂ was very probably consumed in some part of the biofilm, leaving other parts in
 552 strict anaerobic conditions more favorable for acetogenic bacteria growth.

553 The H₂ recovered in the headspace of the PCE accounted for 12 to 22% of the electrons supplied to the
 554 cathode as presented in Table 3. Therefore, H₂ was not related to the biological activity and mostly resulted
 555 from an abiotic reaction at the cathode. In addition, in presence of O₂ in the cathodic chamber, oxygen
 556 reduction reactions were expected with regards to the potential used in this study. Indeed, a two-electron
 557 reduction could have occurred, resulting in the production of hydrogen peroxide (H₂O₂), which can then
 558 undergo further reduction to form water (H₂O) (Rozendal et al., 2009; Sim et al., 2015). Hydrogen peroxide
 559 was not measured, however, the amount of biomass found on the cathodes (Figure 4) suggested that the
 560 concentrations of hydrogen peroxide were sufficiently low to have minimal to no impact on the microbial
 561 community during the enrichment process. Nonetheless, a fraction of the electrons may have been lost
 562 through these oxygen reduction reactions, which could partially account for the low coulombic efficiencies
 563 observed in this study. Interestingly, a significant production of acetate was also observed. An average rate
 564 of 149.1 μmol/L.d and 421.6 μmol/L.d were measured in both PCE for the period from day 131 to day 214,
 565 as presented in Table 3. Acetate production almost stopped with the power failures with acetate measured
 566 only on one to two batches per PCE. This decrease correspond to rate of 61.0 μmol/L.d and 57.4 μmol/L.d
 567 of acetate in both PCE. Acetate production accounted for 7.9 and 39% of the cathodic electrons during the
 568 first period (up to 214 days) and for less than 5% after power failures. To explain the decrease in acetate
 569 production, biomass growth and power consumption, it was hypothesized that acetate production might
 570 have been due to a specific loss of members able to fix CO₂, and more especially autotrophic bacteria using
 571 cathode as electron source (H₂ or DET), within the enriched community. Thus, with acetate no longer being
 572 produced, heterotrophic bacteria did not have enough organic C to sustain their growth, causing their
 573 decrease. Therefore, autotrophic bacteria responsible for CO₂ fixation and heterotrophic bacteria that
 574 could also be H₂ dependent for N₂ fixation were greatly affected, leading to a decrease in the reduction
 575 reactions at the cathode and subsequently in current density. In addition, acetate was not found in the H₂E
 576 bottles, indicating the absence of acetogenesis and an important difference in microbial pathways and/or
 577 communities. As seen in the Table 3, electrons were retrieved in biomass production, N₂ fixation products,
 578 H₂ found in headspace and in CH₃COOH product from CO₂. These products were not sufficient to close the
 579 electron mass balance. The loss of electrons and the differences between cathodes of PCE 1 and PCE 2 was
 580 explained by side reactions, such as O₂ reduction or biological reaction such as exopolysaccharide (EPS)
 581 production.

582 **Table 3** - Current densities, rates and coulombic efficiencies for the two polarized cathode enrichment (PCE) over two
 583 different periods of current density with CO₂ as sole carbon source. During the first period (131-214 days) current density
 584 increased, whereas during the second period (>215) current density decreased after several power outages (see Figure 3).

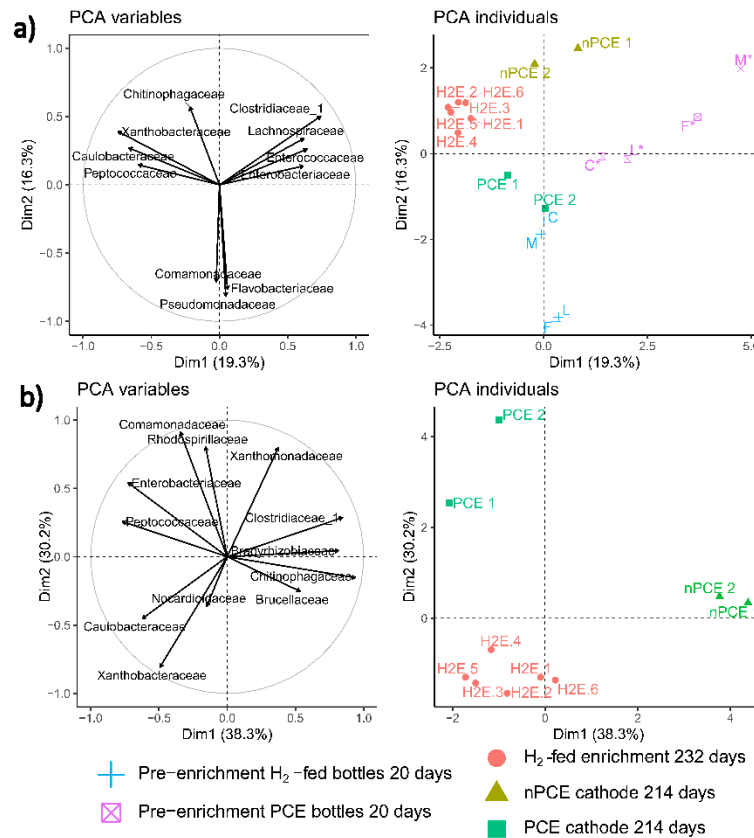
		131-214 days		> 215 days	
		PCE 1	PCE 2	PCE 1	PCE 2
J A/m ²	Mean	7.7±3.1	5.9±2.4	6.2±4.1	3.8±2.2
	Max	28.2	11.3	19.5	9.9
Acetate μmol/L.d	Mean	149.1±203.1	421.6±216.7	57.4±151.8	61.0±106.5
N μmol/L.d	N-NH ₄ ⁺	0.108±0.225	0.155±0.249	2.0±1.4	1.5±1.9
	N Bulk Dry weighth	10.3±6.0	27.5±13.4	9.0±6.4	12.1±6.4
	N Biomass theoretical (16S/bact)	16.7	80.4	-3.0	-7
Biomass bact/L.j	Bulk	0.4 ± 0.5 10 ⁹	3.5 ± 2.0 10 ⁹	0.4±0.5 10 ⁹	0.2±0.1 10 ⁹
	Cathode	0.9 10 ¹⁰	4.6 10 ¹⁰	-2.6±3.5 10 ¹⁰	-5.9±7.8 10 ¹⁰
Coulombic efficiency %	CO ₂ to Acetate	7.9±9.5	30.9±8.9	2.1±5.6	5.0±6.6
	H ⁺ to H ₂	22.3±15.4	12.1±8.8	9.4±13.5	14.4±14.4
	N ₂ fixation	0.6±0.2	3.3±0.8	0.2±1.0	-0.5±2.2
	Biomass growth	2.8±0.5	17.3±5.3	-2.5±4.0	-8.3±14.2
	Total	33.6±14.4	63.6±9.0	9.2±16.5	10.5±18.8

586 In comparison with the other works dealing with N₂-fixing cathodic biofilms, Zhang et al (2022) showed
 587 a maximum of 40.5 mg/L of NH₄⁺ in 4 days with mixed communities, in regard to a maximum of 0.8 mg/L
 588 NH₄⁺ observed in Yadav et al (2022) and 6.31 mg/L NH₄⁺ in 10 days for Li et al. (Li et al., 2022; Yadav et al.,
 589 2022; Zhang et al., 2022). When demonstrating the N₂ fixation in MES, Rago et al (2019) showed a N₂
 590 fixation of 0.2 mgN/L.d in biomass and 5 10⁹ bacteria/L.d (Rago et al., 2019). In the present study, biomass
 591 production in biofilms was 2 to 10 times higher than in Rago et al. (2019), as was the nitrogen found in the
 592 biomass varied between 0.2 and 1 mg/L.d before 214 days (Rago et al., 2019).

593 Microbial communities

594 16S rDNA sequencing was performed at the end of pre-enrichment, and at 214 or 232 days of
 595 enrichment in polarized cathode enrichment (PCE) and in H₂-fed enrichment bottles (H₂E), respectively.
 596 The sampling days were selected because they were associated to a high microbial activity (high current
 597 densities and high biomass concentrations). In H₂E, the *nifH*/16S abundance ratio was also maximum (0.9)
 598 at day 232. Principal Component Analysis (PCA) was used to present the communities for each enrichment.
 599 Each reactors and bottles are presented as individuals and major families as variables in PCA presented in
 600 the Figure 6 and relative abundances are presented in the Figure 7.

601 For communities at the end of the pre-enrichment, the principal component analysis (PCA) showed an
 602 important link between the families of the *Clostridiaceae*, *Enterobacteriaceae*, *Enterococcaceae* and
 603 *Lachnospiraceae* and with the PCE pre-enrichment (Figure 6a). Indeed, the group of communities of pre-
 604 enrichment with organic C is well separated from the others groups and follow the same direction as these
 605 four families. A dominance of the *Enterobacteriaceae* family (mainly of the *Citrobacter* genus) was
 606 observed for each pre-enriched sample expect for the pre-mixed sample where the three others families
 607 are highly present. These families are therefore absent or very weakly represented in the other sequenced
 608 communities as shown in Figure 7.



609

610 **Figure 6** - Results of the principal component analysis (PCA) performed on the microbial communities of a) pre-
 611 enrichments, H₂-fed enrichment bottles (H₂E) after 232 days and cathodes of PCE and nPCE enrichments after 214 days and
 612 b) H₂-fed enrichment bottles (H₂E) after 232 days and cathodes of PCE and nPCE enrichments after 214 days. Only families
 613 of the five major bacterial OTU in each sampled community were used for the analysis. The microbial communities in the

614 pre-enrichment bottles are represented by the following abbreviations: F for forest soil, C for compost, L for the
615 rhizosphere of leguminous plants, and M for a mix of all. Variables least close to the correlation circle are not displayed
616 ($\cos^2 < 0.2$).

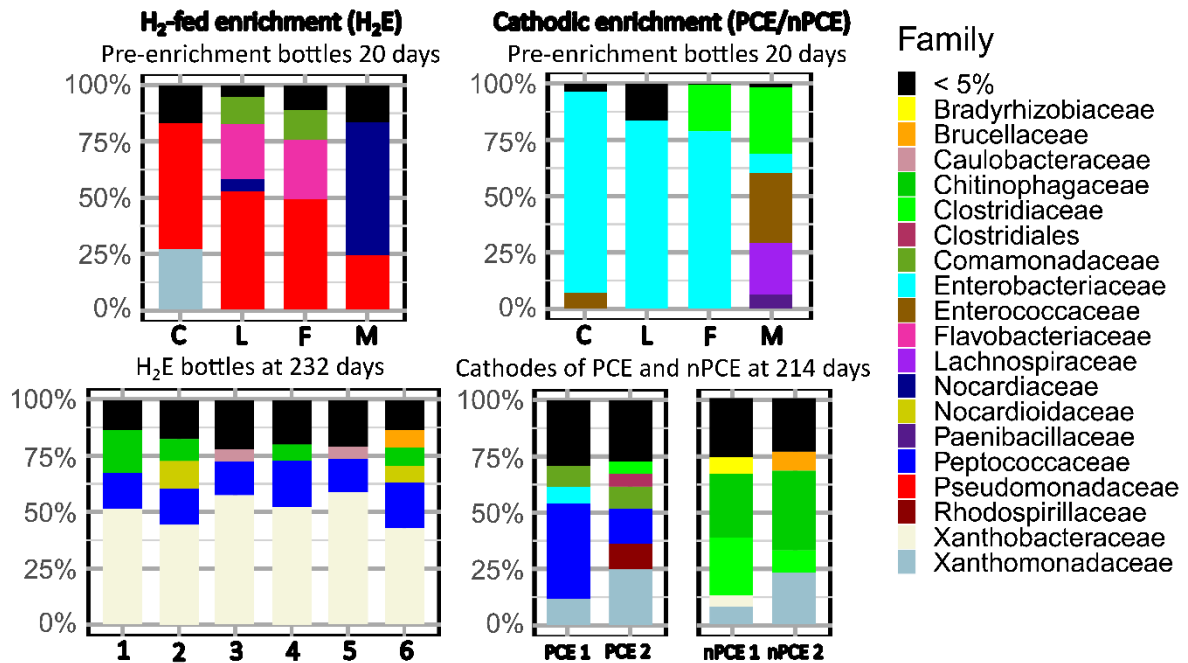
617 For the H₂-fed bottle pre-enrichments (H₂E), the group is also separated of the 232-days enriched
618 community H₂E. *Pseudomonadaceae* (45% of average relative abundance) family was mostly dominant at
619 the end of pre-enrichment. *Nocardiaceae*, *Flavobacteriales*, *Xanthomonadaceae* and *Comamonadaceae*
620 were also present as seen in Figure 7. *Flavobacteriales* and *Comamonadaceae* families are also highly linked
621 with the group of pre-enrichment in PCA of Figure 6a. These families, with the exception of
622 *Flavobacteriales*, are also known to have members possessing the set of genes necessary for N₂ fixation
623 (Dos Santos et al., 2012; Ghodhbane-Gtari et al., 2019; Huda et al., 2022). These families accounted for
624 77% of the sequences which is high compared to the *nifH*/16S rDNA ratio of less than 0.01 at the same time
625 point. This suggests that either the *nifH* primers were not adapted to these specific species or that the
626 species found at this point did not possess the genes for nitrogenases. As the H₂E pre-enrichment cultures
627 started on a medium containing NH₄Cl, the presence of this source of nitrogen was likely favorable to the
628 growth of non-diazotrophic bacteria.

629 After 214 days of enrichment, PCE communities were affiliated to *Peptococcaceae* (29% in average),
630 *Xanthomonadaceae* (18% in average), *Rhodospirillaceae* (11% in PCE 2, *Azospirillum*) and
631 *Comamonadaceae* (10% in average) as presented in Figure 7. As seen in the PCA presented Figure 6b,
632 *Rhodospirillaceae*, *Comamonadaceae*, *Enterobacteriaceae* and *Xanthomonadaceae* families are
633 representative of the PCE cathode communities. *Peptococcaceae* appear to be shared with communities
634 of H₂-fed enrichment (H₂E) bottles. As seen in Figure 6a and Figure 7, a clear shift in microbial communities
635 from the end of pre-enrichment was therefore observed as the difference between PCE communities at
636 214 days and at the end of pre-enrichment.

637 Only *Enterobacteriaceae* family was maintained although at minor relative abundance. Members of
638 *Clostridiales incertae sedis* absent from original inoculum also appeared on polarized cathode. These
639 families are known to exhibit the role of plant growth promoting bacteria (PGPB). These communities could
640 thus be beneficial when used as living fertilizers (Cassan & García de Salamone, 2008; Rojas-Tapias et al.,
641 2012; Singh et al., n.d.). The *Comamonadaceae* as well as the *Enterobacteriaceae* families mostly include
642 heterotrophic species, which would be consistent with our hypotheses about the existence of interactions
643 between heterotrophic and autotrophic populations (F. Liu et al., 2011; Wu et al., 2018). More precisely,
644 the *Peptococcaceae* sequences were affiliated to species *Desulforamulus ruminis* (>98%). This species was
645 already described for their ability to fix N₂ (Postgate, 1970). The *Desulforamulus* and *Desulfotomaculum*
646 genera have also several species able to grow with H₂ and CO₂ as electron and C sources (Aullo et al., 2013;
647 Klemps et al., 1985; Zaybak et al., 2013). They were previously reported to be able to produce acetate by
648 CO₂ reduction through the Calvin cycle (Klemps et al., 1985), and some were already found in microbial
649 electrochemical system on a biocathode producing acetate (Zaybak et al., 2013). The other main family,
650 *Xanthomonadaceae*, was represented by several genera with a majority of *Pseudoxanthomonas*. In this
651 genus, some members were identified as N₂ fixers with a need of external organic C source, exhibiting a
652 mixotrophic metabolism depending on the environmental conditions (J. Hu et al., 2022; Ryan et al., 2009).
653 Sequences associated to the *Rhodospirillaceae* family were mainly affiliated to the species *Azospirillum*
654 *lipoferum* which is able to grow in autotrophy with H₂, CO₂ and N₂ (Tilak et al., 1986). This soil bacterium is
655 also known for its role as a PGPB with a capacity to solubilize phosphates, making it a good candidate as a
656 fertilizer (Cassan & García de Salamone, 2008; Tilak et al., 1986). Interestingly, many of the identified
657 bacteria in the polarized cathode enrichment were previously described to possess the N₂-fixing genes and
658 capability. This supports the fact that the primers were not able to amplify the full diversity of *nifH* genes
659 from these communities.

660 The *Xanthobacteraceae* (51% in average), *Peptococcaceae* (17%, identified as *Desulforamulus*),
661 *Chitinophagaceae* (8%) and *Nocardioidaceae* (5%) families were found to be dominant in H₂E bottles at day
662 214 as presented in Figure 7. The *Xanthobacteraceae* family, highly linked to H₂E communities as seen in
663 Figure 6b, was mostly represented by the species *Xanthobacter autotrophicus* which is known as N₂-fixing
664 HOB (Wiegel, 2005). This species was already been used for N₂ fixation by Liu et al. (C. Liu et al., 2017) in
665 an hybrid system using the H₂ produced by a cathode. *Xanthobacter autotrophicus* was also found in the
666 medium of the polarized cathode enrichment but in lower abundance (< 5%). Therefore, the community

667 enriched with H₂ in bottles was mostly composed of N₂-fixing bacteria, as also supported by the high
 668 *nifH*/16S ratio (0.9). After 214 days of enrichment, diazotrophic HOB were specifically selected.



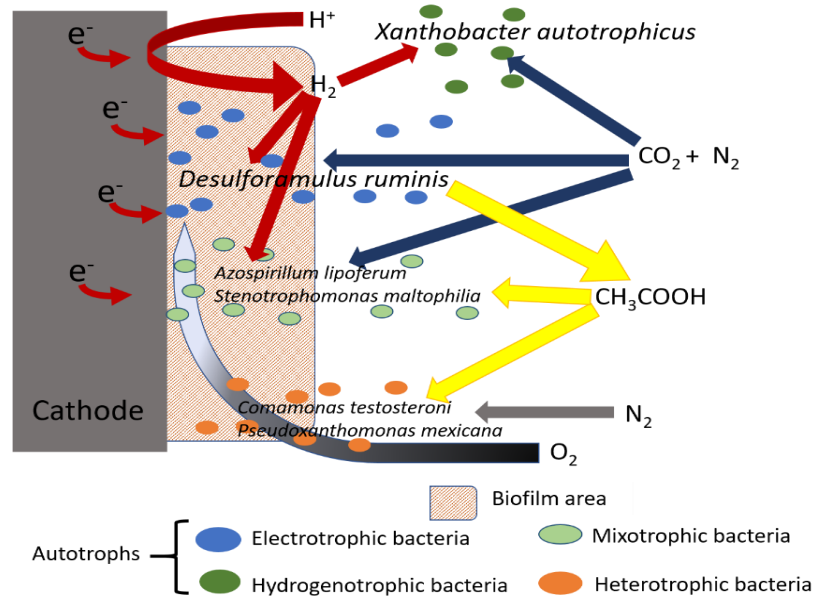
669

670 **Figure 7** - Barplots of relative abundances of major bacterial families of pre-enrichments, of H₂E
 671 after 232 days) and cathodic enrichment (PCE and nPCE after 214 days). The microbial communities in the pre-enrichment
 672 bottles are represented by the following abbreviations: F for forest soil, C for compost, L for the rhizosphere of leguminous
 673 plants, and M for a mix of all. Only families with a relative abundance ≥ 5% are shown for each sample.
 674

675 The presence of mixotrophic and heterotrophic bacteria in the PCE suggested that carbon-based
 676 interactions could have occurred. Acetate was the only abundant soluble carbon metabolite found in these
 677 enrichments (see Table 3). Therefore, acetate was assumed to be used as intermediate for carbon and
 678 electron transfer between autotrophic homoacetogens, e.g. *Desulforamulus rumnis*, and heterotrophic
 679 bacteria such as *Comamonas sp.*).

680 Furthermore the low concentration of N-NH₄⁺ in the PCE before day 210 (Table 3) was probably due to
 681 its rapid consumption for bacteria growth. Considering these hypothesis, a conceptual scheme of microbial
 682 interactions between the main bacterial families in the PCE was proposed and is presented in Figure 8. The
 683 presence of heterotrophic bacteria and their potential use of O₂ as a final electron acceptor was also
 684 considered. The concentration of dissolved O₂ would have decreased in a deep layer of the biofilm due to
 685 its use by heterotrophic bacteria. A structure of the biofilm in two layers could then be proposed with a
 686 first layer composed mainly of homoacetogens fixed on the cathode and reducing CO₂ to acetate, and a
 687 second layer composed mainly of heterotrophic bacteria using acetate and dissolved O₂ to sustain their
 688 growth. It was assumed that bacteria in the first layer would not access to N₂ that would be mostly fixed
 689 by organisms of the second layer.
 690

690



691

692

693

Figure 8 - Conceptual scheme of microbial interactions occurring in polarized cathode enrichment (PCE) after enrichment for N₂ fixation with inorganic energy and carbon sources

694

Conclusion

695

696

697

698

699

700

701

702

703

704

705

706

707

708

709

710

711

712

713

714

715

716

717

718

Enrichment cultures of N₂-fixing bacteria were successfully carried out in H₂-fed bottles (H₂E) and in polarized cathode enrichment (PCE). Both methods showed significant N₂ fixation after 340 days of enrichment. The microbial communities selected were able to fix N₂ with CO₂ as sole carbon source and H₂ or cathodic electrons as sole electron sources. Biomass growth on the cathode up to 4.6 10¹⁰ bacteria/L.d is another evidence of autotrophic growth in the PCE while bacterial growth was much lower in the H₂E. Current density suggests the activity of autotrophic bacteria in the PCE and the availability of electron sources. As the coulombic efficiency of N₂ fixation was low with a maximum of 3.3% and considering the low concentrations of NH₄⁺, it was concluded that the major part of the nitrogen was incorporated into microbial biomass during the enrichment procedure. Interestingly, acetate was also produced in the PCE corresponding to a coulombic efficiency of 27%. The related microbial communities found in both enrichments had some bacterial families in common, but the communities found in the PCE appeared metabolically more diverse, suggesting probable rich microbial interactions with exchanges of electrons, carbon and nitrogen between autotrophic, heterotrophic and mixotrophic populations. Several members of the enriched communities were furthermore reported as plant growth promoting bacteria (PGPB) which could be interesting for the production of environment friendly fertilizers. To summarize, a conceptual model of microbial interactions between the main bacterial families found in the bioelectrochemical system was proposed suggesting a key role of each autotrophic, heterotrophic and mixotrophic populations in the process of N₂ fixing by cathodic biofilms. In order to focus on the enriched microbial community and avoid to disrupt the enrichments, a comprehensive screening with different potential electron acceptors was not performed here. However, such screening would be interesting to be investigated and could be the subject of further studies on synthetic community to further explore the impact of electron acceptors on microbial communities, current densities and coulombic efficiencies.

719

Acknowledgements

720 The authors would like to thank the INRAE Bio2E Facility (Bio2E, INRAE,2018. Environmental
721 Biotechnology and Biorefinery Facility, <https://doi.org/10.15454/1.557234103446854E12>) for
722 experimental support.

723

Data and scripts availability

724 Data and scripts are available online on: <https://doi.org/10.57745/ONNGWZ> (Recherche Data gouv)

725

Conflict of interest disclosure

726 The authors declare that they comply with the PCI rule of having no financial conflicts of interest in
727 relation to the content of the article.

728

Funding

729 This work was funded by the French National Research Agency (ANR, ANR-19-CE43-0013 Cathomix).

730

References

731 Aullo, T., Ranchou-Peyruse, A., Ollivier, B., & Magot, M. (2013). Desulfotomaculum spp. And related
732 gram-positive sulfate-reducing bacteria in deep subsurface environments. *Frontiers in Microbiology*,
733 4. <https://www.frontiersin.org/article/10.3389/fmicb.2013.00362>

734 Bagali, S. (2012). Review: Nitrogen fixing microorganisms. *Int. J. Microbiol. Res.*, 3, 46–52.
735 <https://doi.org/10.5829/idosi.ijmr.2012.3.1.61103>

736 Bergersen, F. J. (1970). The Quantitative Relationship between Nitrogen Fixation and the Acetylene-
737 Reduction Assay. *Australian Journal of Biological Sciences*, 23(4), Article 4.
738 <https://doi.org/10.1071/bi9701015>

739 Bowers, T. H., Reid, N. M., & Lloyd-Jones, G. (2008). Composition of nifH in a wastewater treatment
740 system reliant on N₂ fixation. *Applied Microbiology and Biotechnology*, 79(5), 811–818.
741 <https://doi.org/10.1007/s00253-008-1486-2>

742 Bueno Batista, M., & Dixon, R. (2019). Manipulating nitrogen regulation in diazotrophic bacteria for
743 agronomic benefit. *Biochemical Society Transactions*, 47(2), 603–614.
744 <https://doi.org/10.1042/BST20180342>

745 Burris, R. H., & Roberts, G. P. (1993). Biological Nitrogen Fixation. *Annual Review of Nutrition*, 13(1),
746 Article 1. <https://doi.org/10.1146/annurev.nu.13.070193.001533>

747 Carmona-Martínez, A. A., Trably, E., Milferstedt, K., Lacroix, R., Etcheverry, L., & Bernet, N. (2015).
748 Long-term continuous production of H₂ in a microbial electrolysis cell (MEC) treating saline
749 wastewater. *Water Research*, 81, 149–156. <https://doi.org/10.1016/j.watres.2015.05.041>

750 Cassan, F., & García de Salamone, I. (2008). *Azospirillum: Cell physiology, plant response, agronomic
751 and environmental research in Argentina*. ISBN 978-987-98475-8-9

752 Chakraborty, T., & Akhtar, N. (2021). Biofertilizers: Prospects and Challenges for Future. In
753 *Biofertilizers* (pp. 575–590). John Wiley & Sons, Ltd. <https://doi.org/10.1002/9781119724995.ch20>

- 754 Chen, S., Jing, X., Yan, Y., Huang, S., Liu, X., Chen, P., & Zhou, S. (2020). Bioelectrochemical nitrogen
755 fixation to extracellular ammonium by *Pseudomonas stutzeri*. *Applied and Environmental*
756 *Microbiology*, 87(5). <https://doi.org/10.1128/AEM.01998-20>
- 757 Cherkasov, N., Ibhaden, A. O., & Fitzpatrick, P. (2015). A review of the existing and alternative
758 methods for greener nitrogen fixation. *Chemical Engineering and Processing: Process Intensification*,
759 90, 24–33. <https://doi.org/10.1016/j.cep.2015.02.004>
- 760 Deng, J., Iñiguez, J. A., & Liu, C. (2018). Electrocatalytic Nitrogen Reduction at Low Temperature.
761 *Joule*, 2(5), 846–856. <https://doi.org/10.1016/j.joule.2018.04.014>
- 762 Dos Santos, P. C., Fang, Z., Mason, S. W., Setubal, J. C., & Dixon, R. (2012). Distribution of nitrogen
763 fixation and nitrogenase-like sequences amongst microbial genomes. *BMC Genomics*, 13(1), 162.
764 <https://doi.org/10.1186/1471-2164-13-162>
- 765 Franche, C., Lindström, K., & Elmerich, C. (2009). Nitrogen-fixing bacteria associated with leguminous
766 and non-leguminous plants. *Plant and Soil*, 321(1), 35–59. [https://doi.org/10.1007/s11104-008-](https://doi.org/10.1007/s11104-008-9833-8)
767 [9833-8](https://doi.org/10.1007/s11104-008-9833-8)
- 768 Gaby, J. C., & Buckley, D. H. (2012). A Comprehensive Evaluation of PCR Primers to Amplify the nifH
769 Gene of Nitrogenase. *PLoS ONE*, 7(7), e42149. <https://doi.org/10.1371/journal.pone.0042149>
- 770 Ghodhbane-Gtari, F., Nouioui, I., Hezbri, K., Lundstedt, E., D'Angelo, T., McNutt, Z., Laplaze, L.,
771 Gherbi, H., Vaissayre, V., Svistoonoff, S., Ahmed, H. ben, Boudabous, A., & Tisa, L. S. (2019). The
772 plant-growth-promoting actinobacteria of the genus *Nocardia* induces root nodule formation in
773 *Casuarina glauca*. *Antonie van Leeuwenhoek*, 112(1), 75–90. [https://doi.org/10.1007/s10482-018-](https://doi.org/10.1007/s10482-018-1147-0)
774 [1147-0](https://doi.org/10.1007/s10482-018-1147-0)
- 775 Hardy, R. W. F., Burns, R. C., & Holsten, R. D. (1973). Applications of the acetylene-ethylene assay for
776 measurement of nitrogen fixation. *Soil Biology and Biochemistry*, 5(1), 47–81.
777 [https://doi.org/10.1016/0038-0717\(73\)90093-X](https://doi.org/10.1016/0038-0717(73)90093-X)
- 778 Heldal, M., Norland, S., & Tumyr, O. (1985). X-ray microanalytic method for measurement of dry
779 matter and elemental content of individual bacteria. *Applied and Environmental Microbiology*, 50(5),
780 1251–1257. <https://doi.org/10.1128/aem.50.5.1251-1257.1985>
- 781 Hu, J., Tang, H., Wang, Y. Z., Yang, C., Gao, M., Tsang, Y. F., & Li, J. (2022). Effect of dissolved solids
782 released from biochar on soil microbial metabolism. *Environmental Science: Processes & Impacts*,
783 24(4), 598–608. <https://doi.org/10.1039/D2EM00036A>
- 784 Hu, X., Kerckhof, F.-M., Ghesquière, J., Bernaerts, K., Boeckx, P., Clauwaert, P., & Boon, N. (2020).
785 Microbial Protein out of Thin Air: Fixation of Nitrogen Gas by an Autotrophic Hydrogen-Oxidizing
786 Bacterial Enrichment. *Environmental Science & Technology*, 54(6), Article 6.
787 <https://doi.org/10.1021/acs.est.9b06755>
- 788 Huda, N. ul, Tanvir, R., Badar, J., Ali, I., & Rehman, Y. (2022). Arsenic-Resistant Plant Growth
789 Promoting *Pseudoxanthomonas mexicana* S254 and *Stenotrophomonas maltophilia* S255 Isolated
790 from Agriculture Soil Contaminated by Industrial Effluent. *Sustainability*, 14(17), Article 17.
791 <https://doi.org/10.3390/su141710697>
- 792 Kandemir, T., Schuster, M. E., Senyshyn, A., Behrens, M., & Schlögl, R. (2013). The Haber–Bosch
793 Process Revisited: On the Real Structure and Stability of “Ammonia Iron” under Working Conditions.

- 794 *Angewandte Chemie International Edition*, 52(48), Article 48.
795 <https://doi.org/10.1002/anie.201305812>
- 796 Khan, K. S., Mack, R., Castillo, X., Kaiser, M., & Joergensen, R. G. (2016). Microbial biomass, fungal
797 and bacterial residues, and their relationships to the soil organic matter C/N/P/S ratios. *Geoderma*,
798 271, 115–123. <https://doi.org/10.1016/j.geoderma.2016.02.019>
- 799 Kifle, M. H., & Laing, M. D. (2016). Isolation and Screening of Bacteria for Their Diazotrophic
800 Potential and Their Influence on Growth Promotion of Maize Seedlings in Greenhouses. *Frontiers in*
801 *Plant Science*, 6. <https://doi.org/10.3389/fpls.2015.01225>
- 802 Kim, J., & Rees, D. C. (1994). Nitrogenase and biological nitrogen fixation. *Biochemistry*, 33(2), Article
803 2. <https://doi.org/10.1021/bi00168a001>
- 804 Klemps, R., Cypionka, H., Widdel, F., & Pfennig, N. (1985). Growth with hydrogen, and further
805 physiological characteristics of *Desulfotomaculum* species. *Archives of Microbiology*, 143(2), 203–
806 208. <https://doi.org/10.1007/BF00411048>
- 807 Li, F., Li, F., Lin, Y., Guo, L., Zhang, L., Li, R., Tian, Q., Wang, Y., Wang, Y., Zhang, X., Liu, J., & Fan, C.
808 (2022). Investigating the performance and mechanism of nitrogen gas fixation and conversion to
809 ammonia based on biocathode bioelectrochemistry system. *Journal of Chemical Technology &*
810 *Biotechnology*, 97(8), 2163–2170. <https://doi.org/10.1002/jctb.7092>
- 811 Liu, A., Yang, Y., Ren, X., Zhao, Q., Gao, M., Guan, W., Meng, F., Gao, L., Yang, Q., Liang, X., & Ma, T.
812 (2020). Current Progress of Electrocatalysts for Ammonia Synthesis Through Electrochemical
813 Nitrogen Reduction Under Ambient Conditions. *ChemSusChem*, 13(15), 3766–3788.
814 <https://doi.org/10.1002/cssc.202000487>
- 815 Liu, C., Sakimoto, K. K., Colón, B. C., Silver, P. A., & Nocera, D. G. (2017). Ambient nitrogen reduction
816 cycle using a hybrid inorganic–biological system. *Proceedings of the National Academy of Sciences*,
817 114(25), Article 25. <https://doi.org/10.1073/pnas.1706371114>
- 818 Liu, F., Zhao, C., Xia, L., Yang, F., Chang, X., & Wang, Y. (2011). Biofouling characteristics and
819 identification of preponderant bacteria at different nutrient levels in batch tests of a recirculating
820 cooling water system. *Environmental Technology*, 32(8), 901–910.
821 <https://doi.org/10.1080/09593330.2010.517220>
- 822 Loferer-Krößbacher, M., Klima, J., & Psenner, R. (1998). Determination of Bacterial Cell Dry Mass by
823 Transmission Electron Microscopy and Densitometric Image Analysis. *Applied and Environmental*
824 *Microbiology*, 64(2), 688–694. <https://doi.org/10.1128/AEM.64.2.688-694.1998>
- 825 Logan, B. E., Rossi, R., Ragab, A., & Saikaly, P. E. (2019). Electroactive microorganisms in
826 bioelectrochemical systems. *Nature Reviews Microbiology*, 17(5), Article 5.
827 <https://doi.org/10.1038/s41579-019-0173-x>
- 828 Martín, A. J., Shinagawa, T., & Pérez-Ramírez, J. (2019). Electrocatalytic Reduction of Nitrogen: From
829 Haber-Bosch to Ammonia Artificial Leaf. *Chem*, 5(2), Article 2.
830 <https://doi.org/10.1016/j.chempr.2018.10.010>
- 831 Masclaux-Daubresse, C., Daniel-Vedele, F., Dechorgnat, J., Chardon, F., Gaufichon, L., & Suzuki, A.
832 (2010). Nitrogen uptake, assimilation and remobilization in plants: Challenges for sustainable and
833 productive agriculture. *Annals of Botany*, 105(7), 1141–1157. <https://doi.org/10.1093/aob/mcq028>

- 834 McMurdie, P. J. (2023). *Phyloseq* [R]. <https://github.com/joey711/phyloseq> (Original work published
835 2011)
- 836 Moscoviz, R., Desmond-Le Quéméner, E., Trably, E., & Bernet, N. (2019). Bioelectrochemical Systems
837 for the Valorization of Organic Residues. In J.-R. Bastidas-Oyanedel & J. E. Schmidt (Eds.), *Biorefinery:
838 Integrated Sustainable Processes for Biomass Conversion to Biomaterials, Biofuels, and Fertilizers*
839 (pp. 511–534). Springer International Publishing. https://doi.org/10.1007/978-3-030-10961-5_21
- 840 Paul, D., Noori, M. T., Rajesh, P. P., Ghangrekar, M. M., & Mitra, A. (2018). Modification of carbon
841 felt anode with graphene oxide-zeolite composite for enhancing the performance of microbial fuel
842 cell. *Sustainable Energy Technologies and Assessments*, 26, 77–82.
843 <https://doi.org/10.1016/j.seta.2017.10.001>
- 844 Peoples, M. B., & Craswell, E. T. (1992). Biological nitrogen fixation: Investments, expectations and
845 actual contributions to agriculture. *Plant and Soil*, 141(1), 13–39.
846 <https://doi.org/10.1007/BF00011308>
- 847 Pogoreutz, C., Rädercker, N., Cárdenas, A., Gärdes, A., Wild, C., & Voolstra, C. R. (2017). Nitrogen
848 Fixation Aligns with nifH Abundance and Expression in Two Coral Trophic Functional Groups.
849 *Frontiers in Microbiology*, 8. <https://www.frontiersin.org/articles/10.3389/fmicb.2017.01187>
- 850 Poly, F., Ranjard, L., Nazaret, S., Gourbière, F., & Monrozier, L. J. (2001). Comparison of nifH Gene
851 Pools in Soils and Soil Microenvironments with Contrasting Properties. *Applied and Environmental
852 Microbiology*, 67(5), 2255–2262. <https://doi.org/10.1128/AEM.67.5.2255-2262.2001>
- 853 Postgate, J. R. (1970). Nitrogen Fixation by Sporulating Sulphate-reducing Bacteria Including Rumen
854 Strains. *Microbiology*, 63(1), 137–139. <https://doi.org/10.1099/00221287-63-1-137>
- 855 Rago, L., Zecchin, S., Villa, F., Goglio, A., Corsini, A., Cavalca, L., & Schievano, A. (2019).
856 Bioelectrochemical Nitrogen fixation (e-BNF): Electro-stimulation of enriched biofilm communities
857 drives autotrophic nitrogen and carbon fixation. *Bioelectrochemistry*, 125, 105–115.
858 <https://doi.org/10.1016/j.bioelechem.2018.10.002>
- 859 Rojas-Tapias, D., Moreno-Galván, A., Pardo-Díaz, S., Obando, M., Rivera, D., & Bonilla, R. (2012).
860 Effect of inoculation with plant growth-promoting bacteria (PGPB) on amelioration of saline stress in
861 maize (*Zea mays*). *Applied Soil Ecology*, 61, 264–272. <https://doi.org/10.1016/j.apsoil.2012.01.006>
- 862 Rozendal, R. A., Leone, E., Keller, J., & Rabaey, K. (2009). Efficient hydrogen peroxide generation
863 from organic matter in a bioelectrochemical system. *Electrochemistry Communications*, 11(9), 1752–
864 1755. <https://doi.org/10.1016/j.elecom.2009.07.008>
- 865 Ryan, R. P., Monchy, S., Cardinale, M., Taghavi, S., Crossman, L., Avison, M. B., Berg, G., van der Lelie,
866 D., & Dow, J. M. (2009). The versatility and adaptation of bacteria from the genus
867 *Stenotrophomonas*. *Nature Reviews Microbiology*, 7(7), Article 7.
868 <https://doi.org/10.1038/nrmicro2163>
- 869 Sim, J., An, J., Elbeshbishy, E., Ryu, H., & Lee, H.-S. (2015). Characterization and optimization of
870 cathodic conditions for H₂O₂ synthesis in microbial electrochemical cells. *Bioresource Technology*,
871 195, 31–36. <https://doi.org/10.1016/j.biortech.2015.06.076>
- 872 Singh, R. K., Singh, P., Li, H.-B., Guo, D.-J., Song, Q.-Q., Yang, T., Malviya, M. K., Song, X.-P., & Li, Y.-R.
873 (2020). Plant-PGPR interaction study of plant growth-promoting diazotrophs *Kosakonia radicincitans*
874 BA1 and *Stenotrophomonas maltophilia* COA2 to enhance growth and stress-related gene

- 875 expression in *Saccharum* spp. *Journal of Plant Interactions*, 15,427-445.
876 <https://doi.org/10.1080/17429145.2020.1857857>
- 877 Soundararajan, M., Ledbetter, R., Kusuma, P., Zhen, S., Ludden, P., Bugbee, B., Ensign, S. A., &
878 Seefeldt, L. C. (2019). Phototrophic N₂ and CO₂ Fixation Using a *Rhodospseudomonas palustris*-H₂
879 Mediated Electrochemical System With Infrared Photons. *Frontiers in Microbiology*, 10, 1817.
880 <https://doi.org/10.3389/fmicb.2019.01817>
- 881 Stoddard, S. F., Smith, B. J., Hein, R., Roller, B. R. K., & Schmidt, T. M. (2015). rrnDB: Improved tools
882 for interpreting rRNA gene abundance in bacteria and archaea and a new foundation for future
883 development. *Nucleic Acids Research*, 43(D1), D593–D598. <https://doi.org/10.1093/nar/gku1201>
- 884 Temple, S. J., Vance, C. P., & Stephen Gantt, J. (1998). Glutamate synthase and nitrogen assimilation.
885 *Trends in Plant Science*, 3(2), 51–56. [https://doi.org/10.1016/S1360-1385\(97\)01159-X](https://doi.org/10.1016/S1360-1385(97)01159-X)
- 886 Tidyverse. (n.d.). Retrieved 9 February 2023, from <https://www.tidyverse.org/>
- 887 Tilak, K. V. B. R., Schneider, K., & Schlegel, H. G. (1986). Autotrophic growth of nitrogen-
888 fixing *Azospirillum* species and partial characterization of hydrogenase from strain CC. *Current*
889 *Microbiology*, 13(6), 291–297. <https://doi.org/10.1007/BF01577194>
- 890 Wiegel, J. (2005). *Xanthobacter Wiegel, Wilke, Baumgarten, Opitz and Schlegel 1978, 573 AL.*
891 https://doi.org/10.1007/0-387-29298-5_135
- 892 Wresta, A., Widayarni, R., Boopathy, R., & Setiadi, T. (2021). Thermodynamic approach to estimating
893 reactions and stoichiometric coefficients of anaerobic glucose and hydrogen utilization. *Engineering*
894 *Reports*, 3(6), e12347. <https://doi.org/10.1002/eng2.12347>
- 895 Wu, Y., Zaiden, N., & Cao, B. (2018). The Core- and Pan-Genomic Analyses of the Genus *Comamonas*:
896 From Environmental Adaptation to Potential Virulence. *Frontiers in Microbiology*, 9, 3096.
897 <https://doi.org/10.3389/fmicb.2018.03096>
- 898 y. Hafeez, F., yasmin, S., Ariani, D., Renseigné, N., Zafar, yusuf, & A. Malik, K. (2006). Plant growth-
899 promoting bacteria as biofertilizer. *Agronomy for Sustainable Development*, 26(2), 143–150.
900 <https://doi.org/10.1051/agro:2006007>
- 901 Yadav, R., Chiranjeevi, P., Yadav, S., Singh, R., & Patil, S. A. (2022). Electricity-driven bioproduction
902 from CO₂ and N₂ feedstocks using enriched mixed microbial culture. *Journal of CO₂ Utilization*, 60,
903 101997. <https://doi.org/10.1016/j.jcou.2022.101997>
- 904 Zaybak, Z., Pisciotta, J. M., Tokash, J. C., & Logan, B. E. (2013). Enhanced start-up of anaerobic
905 facultatively autotrophic biocathodes in bioelectrochemical systems. *Journal of Biotechnology*,
906 168(4), 478–485. <https://doi.org/10.1016/j.jbiotec.2013.10.001>
- 907 Zhang, L., Tian, C., Wang, H., Gu, W., Zheng, D., Cui, M., Wang, X., He, X., Zhan, G., & Li, D. (2022).
908 Improving electroautotrophic ammonium production from nitrogen gas by simultaneous carbon
909 dioxide fixation in a dual-chamber microbial electrolysis cell. *Bioelectrochemistry (Amsterdam,*
910 *Netherlands)*, 144, 108044. <https://doi.org/10.1016/j.bioelechem.2021.108044>
- 911